Sotagliflozin ameliorates doxorubicin-induced cardiomyopathy by regulating inflammation and mitochondrial dysfunction through the AMPK/mTOR pathway

HAIFENG LIU[1], DANYE HAN[2] and MEILING LI[3]

[1]Department of Hematology, Anhui Zhongke Gengjiu Hospital, Hefei, Anhui 230000, P.R. China; [2]Department of Respiratory Medicine, Fuyang Hospital of Anhui Medical University, Fuyang, Anhui 236000, P.R. China; [3]Department of Hematology, The Second Affiliated Hospital of Fujian Medical University, Quanzhou, Fujian 362000, P.R. China

Received June 5, 2025; Accepted January 12, 2026

DOI: 10.3892/etm.2026.13201

Abstract. Sodium-glucose co-transport protein inhibitor Sotagliflozin (SOTA) has demonstrated cardiovascular benefits in diabetic patients, while doxorubicin (DOX) is widely used to generate cardiomyopathy experimental models. The present study investigated the cardioprotective mechanisms of SOTA on DOX-induced heart failure *in vitro* and *in vivo*. First, C57BL/6 mice were injected with multiple doses of DOX (total 15 mg/kg), and the *in vivo* impact of SOTA on cardiac function and cardiomyopathy-related biochemical signaling was assessed. Next, H9C2 cells were treated with DOX in the presence of SOTA to examine the changes in cell viability, mitochondrial function, inflammation, oxidative stress and cell death-related signal pathways. SOTA treatment *in vivo* alleviated cardiac dysfunction and fibrosis while reducing cardiomyocyte apoptosis, inflammation, oxidative stress and mitochondrial dysfunction. *In vitro,* H9c2 cells exposed to DOX in the presence of SOTA exhibited enhanced cell viability and mitigated apoptosis, inflammation, oxidative stress and mitochondrial damage. Furthermore, cleaved caspase-3 and inflammatory cytokine (IL-6, IL-1β and TNF-α) levels were decreased. Reactive oxygen species and mitochondrial Ca^{2+} loading were reduced. Mitochondrial dysfunction was also improved, as indicated by increased JC-1 aggregates and Bcl-2/Bax ratios. Notably, SOTA activated 5' AMP-activated protein kinase (AMPK) and inhibited mTOR signaling while protecting from DOX-induced cardiomyopathy, suggesting SOTA as a promising therapeutic for heart failure treatment.

Correspondence to: Dr Meiling Li, Department of Hematology, The Second Affiliated Hospital of Fujian Medical University, 34 Zhongshan North Road, Quanzhou, Fujian 362000, P.R. China
E-mail: limeiling666@126.com

Key words: sotagliflozin, doxorubicin, cardiomyopathy, apoptosis, inflammation, mitochondrial dysfunction, 5' AMP-activated protein kinase, mTOR, signal transduction pathway

Introduction

Doxorubicin (DOX) is a known anti-tumor drug used to treat numerous malignancies, including breast, prostate and urothelial, thyroid and gall bladder cancer (1). However, its use is limited by its notable cardiotoxicity, which may lead to cardiomyopathy or arrhythmias. DOX-induced cardiomyopathy, which is very similar to dilated cardiomyopathy, is a lethal disease that potentially leads to heart failure or even mortality (2). Multiple mechanisms are involved in DOX-induced myocardial toxicity, including topoisomerase II inhibition, increased oxidative stress, lipid peroxidation, altered calcium homeostasis, inflammation, mitochondrial dysfunction and ultimately cell necrosis, apoptosis and autophagy (3,4). Oxidative stress and inflammation serve notable roles in DOX-induced myocardial toxicity (5,6). The high affinity between DOX and cardiolipin, a membrane phospholipid that resides in the inner face of the mitochondrial membrane in cardiomyocytes, results in DOX accumulation in mitochondria and mitochondrial dysfunction, which is mediated by oxidative stress and leads to the interruption of the electron transfer chain by inhibiting the activity of complexes I, II and IV (7-9). Furthermore, DOX can also cause mitochondrial dysfunction through peroxisome proliferator-activated receptor (PPAR), activating oxidative stress and inflammation and ultimately inducing apoptosis. DOX can reduce PPAR expression by regulating sirtuin 1 (SIRT1) or 5' AMP-activated protein kinase (AMPK) signaling and by upregulating NF-κB expression and thus, promoting inflammatory factor release and worsening of the inflammatory response (10). Conversely, DOX can also decrease nuclear factor erythroid 2-related factor 2 (Nrf2) expression through PPAR inhibition and thereby reduce the levels of antioxidant enzymes and antioxidant capacity, contributing to an oxidative stress response (11). Furthermore, oxidative stress and inflammatory responses are mutually causal and promote each other, exacerbating DOX-induced cardiomyopathy. Inflammatory cytokines can participate in the generation of reactive oxygen species (ROS). Simultaneously, ROS can induce NF-κB nuclear transcription factor activation and indirectly increase the level of inflammatory factors, resulting in their upregulation, thus aggravating

the inflammatory response. Numerous studies have shown that oxidative stress and inflammation are closely associated with DOX-induced cardiomyopathy (3-9). To sustain the prolonged use of DOX as an anticancer treatment, developing pharmacological strategies with cardioprotective effects against DOX-induced cardiotoxicity is necessary.

Sotagliflozin (SOTA) is an oral inhibitor of sodium-glucose co-transport proteins (SGLT) 1 and 2, which reduce blood glucose levels. SOTA is effective in decreasing the likelihood of cardiovascular events in patients diagnosed with either type 1 or type 2 diabetes (12). The Effect of Sotagliflozin on Cardiovascular Events in Patients with Type 2 Diabetes Post Worsening Heart Failure (SOLOIST-WHF) trial evaluated the efficacy of SOTA in treating acute heart failure in patients with type 2 diabetes and heart failure. Patients treated with SOTA experienced fewer cardiovascular-related mortalities, fewer heart failure-related hospitalizations and emergency visits compared with the placebo group, with no notable difference in major adverse events (13). In addition, the Effect of Sotagliflozin on Cardiovascular and Renal Events in Patients with Type 2 Diabetes and Moderate Renal Impairment Who Are at Cardiovascular Risk (SCORED) trial monitored 10,584 participants treated with SOTA or placebo for 16 months. Study endpoints, including cardiovascular-related mortalities, heart failure-related hospitalizations and emergency visits, occurred in 5.6% of the SOTA group and in 7.5% of the placebo group. Furthermore, SOTA lowered the risk of major adverse cardiovascular events by 16% (14). Overall, in patients with type 2 diabetes and chronic kidney disease, SOTA notably decreased the likelihood of cardiovascular events.

Previous studies have demonstrated that SGLT2 inhibitors exhibit multiple pathways for treating heart failure, including reducing cardiac workload, inhibiting inflammation and oxidative stress and improving energy metabolism. SGLT2 inhibitors reduce blood pressure and overall body weight, thus alleviating heart workload and oxygen consumption. Furthermore, SGLT2 inhibitors decrease the release of inflammatory factors from adipose tissue while inhibiting inflammatory reactions and oxidative stress in the heart, ultimately protecting cardiomyocytes. Lastly, SGLT2 inhibitors improve energy metabolism, inhibiting the onset and development of cardiac fibrosis and preventing ventricular remodeling as well as functional deterioration (15,16).

Recent research has revealed a spectrum of effects that extend beyond glucose regulation, demonstrating the therapeutic potential of SGLT1/2 inhibitors in non-diabetic settings (17). In preclinical studies (17-19), SGLT2 inhibitors have been shown to mitigate cardiac inflammation and fibrosis through the modulation of key signaling pathways, such as NF-κB and the NLR family pyrin domain containing 3 (NLRP3) inflammasome, even in the absence of diabetes (17) and through reduced levels of proinflammatory cytokines, including TNF-α and interleukins. The SGLT2 inhibitors empagliflozin and dapagliflozin reduced NLRP3 inflammasome activation and the expression of inflammatory mediators, with efficacy noted in both *in vivo* and *in vitro* environments (18,19). SGLT2 inhibitors attenuated the generation of ROS and enhanced endogenous antioxidant mechanisms in models such as non-diabetic mice subjected to pressure overload-induced heart failure. These effects were replicated in isolated cardiomyocytes from mice on high-fat diets and under conditions of hypoxia/reoxygenation (18,20). Dapagliflozin protected H9c2 rat cardiomyoblasts from DOX-induced cytotoxicity by inhibiting the toll-like receptor 4 (TLR4)/NLRP3/NF-κB inflammatory pathway, which is independent of glycemic modulation (19).

Although the majority of published data refers to SGLT2 inhibitors as a class, the dual mechanism of SOTA (targeting both SGLT1 and SGLT2) raises the possibility of even broader effects due to contributions from SGLT1 inhibition. However, direct studies of SOTA in comparable non-diabetic preclinical cardiac models remain an area warranting continued study.

Beyond its cardiovascular benefits, SOTA has been investigated within the context of cancer, including non-diabetic models of pancreatic malignancy. Preclinical evidence reveals a mechanistic basis for anti-tumor activity of SOTA. In pancreatic cancer cell lines (PANC-1 and BxPC-3), SGLT2 inhibition was shown to promote cancer progression by activating the Hippo signaling pathway through the heterogeneous nuclear ribonucleoprotein K (hnRNPK)/yes-associated protein 1 (YAP1) axis. SOTA, through its SGLT2 inhibition, effectively suppressed the proliferation and invasion of these pancreatic cancer cells (21). By blocking the hnRNPK/YAP1 signaling axis, SOTA interferes with key processes driving tumor growth, indicating a potential role in oncology, independent of glucose regulation (21). Unique to SOTA, SGLT1 inhibition may provide further benefits in tissues where SGLT1 is expressed, such as the myocardium and intestine, but this remains to be fully elucidated in non-diabetic contexts.

SGLT2 inhibitors have already gained approval for heart failure management regardless of diabetes status. The dual SGLT1/2 inhibition of SOTA offers incremental advantages, especially in conditions marked by inflammation or oxidative stress (17). The observed anti-proliferative effects in pancreatic cancer models warrant further investigation into SOTA as a possible adjunct treatment in oncology (21). Finally, given the modulation of inflammatory signaling, SOTA may be relevant for other diseases characterized by chronic inflammation or fibrosis, such as diabetes and cardiovascular diseases (19).

Although the mechanism of action of SGLT2 inhibitors in heart failure has been partially studied in diabetic patients, the specific mechanism of the dual-SGLT inhibitor SOTA in heart failure has not been fully elucidated. SOTA can alleviate cardiac damage by activating the TLR4/calcium/calmodulin-dependent protein kinase II (CaMKII) pathway (22) and by ameliorating angiotensin II (Ang II)-induced oxidative stress and senescence (23). SOTA also attenuates ROS generation and inflammatory cytokine levels in coronary endothelial cells (24,25). However, the specific mechanisms induced by SOTA in non-diabetic cardiomyopathy, particularly DOX-induced cardiomyopathy, remain unclear.

The present study investigated the cardioprotective properties of SOTA on DOX-induced cardiomyopathy and elucidated its underlying mechanisms. The present study evaluated the cardioprotective effects of SOTA by evaluating its effects on apoptosis, inflammation and myocardial function using both *in vitro* and *in vivo* models of DOX-induced cardiomyopathy. The present study aimed to provide evidence supporting the potential application of SOTA as a cardioprotective agent for

DOX-induced cardiac dysfunction and reveal its underlying mechanisms for the treatment of heart failure.

Materials and methods

Animals and treatments. Animal experimentation practices adhered to the Animal Research: Reporting of *In Vivo* Experiments guidelines (26) and the National Research Council's Guide for the Care and Use of Laboratory Animals (26). The Animal Experimental Research Ethics Committee at Fujian Medical University (Fujian, China) approved the present study (approval no. 599). A total of 18 C57BL/6 male mice (6 weeks old; 20±2 g) were acquired from GemPharmatech Co., Ltd. Before commencing the experiment, mice were accommodated in a specific pathogen-free environment with standard laboratory conditions, including a 12-h light/dark cycle, a temperature of 20-25˚C and a humidity of 50±5%, with *ad libitum* access to food and water for 7 days to acclimate to the environment. To investigate the cardioprotective effects of sotagliflozin, a DOX-induced acute cardiotoxicity model was used, following a previous protocol (4,5) and predefined humane endpoints, including severe weight loss (>20%), prostration, cachexia signs, peritoneal/pleural effusion or severe congestive heart failure. Unlike chronic heart failure models that require months to develop, the DOX model induces rapid and severe pathological changes, including myocardial fiber rupture, apoptosis and inflammation, within a short timeframe. This acute progression makes it highly suitable for evaluating the efficacy of short-term therapeutic interventions. Each one of the 18 mice were allocated randomly into three groups (n=6/group): Control, SOTA alone and SOTA + DOX. The control group received an intraperitoneal injection of saline for 10 days. For the DOX group, mice received an equal volume of saline by oral gavage for the first 3 days as a vehicle control for SOTA, followed by DOX intraperitoneal administration (2.17 mg/kg/day) for 7 consecutive days (the total DOX dose was 15 mg/kg). For all experiments, SOTA was administered concurrently with DOX. The DOX + SOTA group received SOTA 30 mg/kg/day alone through oral gavage for the first 3 days, which was then combined with treatment with the same concentrations of DOX as the DOX alone group through intraperitoneal injection for the last 7 days, for a total of 10 days of treatment. The mice were observed daily and their body weight was tracked every 2 days. On day 10, an echocardiography was performed, followed by euthanasia with an overdose of sodium pentobarbital (200 mg/kg through intraperitoneal injection). Blood samples were then collected from the abdominal aorta for further analysis. The murine hearts were excised, fixed in 10% formaldehyde and stored at -80˚C until the assays were performed. Throughout the experiment, randomization procedures and blinded methods were employed.

Transthoracic echocardiography. On day 10, cardiac function and representative motion (M)-mode echocardiography images in 1.5% isoflurane-anesthetized mice were assessed by echocardiography using the VisualSonics Vevo® 2100 imaging system (Visual Sonics, Inc.). M-mode echocardiography was used to calculate left ventricular fractional shortening rate (LVFS), left ventricular ejection fraction (LVEF), left ventricular volume in systole (LV Vol s), left ventricular volume in diastole (LV Vol d), left ventricular internal dimensions in systole (LVIDs), left ventricular internal dimensions in diastole (LVIDd) and the early/atrial (E/A) ratio using Vevo analysis software (version 5.8.0; FUJIFILM; Visual Sonics, Inc.). Parameters and averages were calculated for ≥5 consecutive cardiac cycles.

H&E staining. Heart tissue from model mice was collected and evaluated with the Hematoxylin and Eosin Staining Kit (C0105S; Beyotime Biotechnology) according to the manufacturer's instructions. Briefly, the heart tissue was fixed in 10% formaldehyde at room temperature for 48 h and dehydrated in 30% sucrose, before tissues were sliced into 5-μm sections and hematoxylin staining was performed (5 min at room temperature). The stained tissues were dehydrated for 10 min each in 70% and 90% alcohol, before eosin stain was added (1-2 min at room temperature). Next, after dehydrating the stained sections with pure alcohol and xylene and subsequently sealing with neutral resin, images were taken under a light microscope (Olympus BX53; Olympus Corporation).

Sirius red staining. Myocardial fibrosis in mouse cardiac tissue was assessed using the Sirius Red Stain Kit (cat. no. G1470; Beijing Solarbio Science & Technology Co., Ltd.). Briefly, the paraffin-embedded tissues were processed and sections (6 μm) were prepared following previous protocol (5). The sections were then added to a saturated solution of picric acid in distilled water containing 0.1% Sirius Red F3BA and 0.1% Fast Green FCF (Polysciences, Inc.) and incubated at room temperature for 30 min. Finally, the sections were mounted in neutral gum and images were captured under polarized light microscopy.

Cell viability. H9c2 cells were obtained from Procell Life Science & Technology Co., Ltd. The cells were incubated (37˚C and 5% CO_2) in DMEM (cat. no. C2701; Beyotime Biotechnology) containing 1% streptomycin/penicillin and 10% FBS (cat. no. C0232; Gibco; Thermo Fisher Scientific, Inc.). Cells were seeded in a humidified incubator with 5% CO_2 at 37˚C. After 24 h of cell culture, H9c2 cells were treated with different concentrations of SOTA (0, 5, 10, 20 and 40 μM; to determine the optimal SOTA concentration) and cultured for 12 h, in the presence or absence of DOX (10 μM), SOTA and DOX were both purchased from Shanghai Yuanye Bio-Technology Co., Ltd. For separate AMPK/mTOR signaling pathway inhibitor experiments, cells were concomitantly administered DOX and SOTA with 10 μM Compound C (cat. no. ab120843; Abcam).

Cell Counting Kit-8 (CCK-8) cell viability assay. A CCK-8 assay was used to determine cell viability. After the appropriate culture period, 10 μl CCK-8 solution (cat. no. C0037; Beyotime Biotechnology) was added to each well and the culture was incubated for 1 h. The absorbance was measured at 450 nm using the Wuxi Huawei Diatek microplate reader (DR-3518G; Wuxi Huawei Diatek Instrument Co., Ltd.).

Measurement of intracellular ROS. A ROS detection kit (cat. no. HR8821; Beijing Solarbio Science & Technology Co., Ltd.)

was used according to the manufacturer's instructions to determine total intracellular ROS levels. Briefly, cells were incubated (37˚C and 5% CO_2 for 24 h) with fresh medium before 10 μM of diluted (1:1,000) 2',7'-dichlorodihydrofluorescein diacetate (DCFH-DA) probe was added, followed by incubation for 30 min at 37˚C in a 5% CO_2 incubator. Next, the probes were washed three times in DMEM solution without FBS. The intracellular fluorescence intensity was detected using the Olympus BX 53 fluorescence microscope (Olympus Corporation).

Detection of mitochondrial membrane potential. The mitochondrial membrane potential assay kit with JC-1 (cat. no. C2006; Beyotime Biotechnology) was used according to the manufacturer's protocols to detect the mitochondrial membrane potential. Specifically, H9c2 cells seeded on slides were mixed with 1 ml JC-1 staining working solution, incubated for 20 min at 37˚C in a cell incubator and then washed with 5-fold diluted JC-1 staining buffer. DAPI staining solution was added dropwise and incubated for 10 min at room temperature protected from light. Finally, images were captured using the Olympus BX 53 fluorescence microscope (Olympus Corporation).

Detection of mitochondrial calcium (Ca^{2+}) levels. A fluorescent probe Rhod2-AM (Beijing Biolab Technology Co., Ltd.) was used to detect relative Ca^{2+} levels in mitochondria. Specifically, a working solution containing 10 μM Rhod2-AM, 0.25% DMSO and 0.02% Pluronic F-127 (cat. no. KM0188; Beijing Biolab Technology Co., Ltd.) was prepared. H9c2 cells were cultured on slides ($5x10^5$/well) incubated in serum-free phenol red-free medium in 24-well plates; the Rhod2-AM working solution was added to cover the cells and they were incubated for 20 min at 37˚C. The excess staining working solution was rinsed off and DAPI staining solution was added dropwise and incubated for 10 min at room temperature protected from light. Finally, images were captured using the UltraVIEW VoX confocal microscope system (PerkinElmer, Inc.).

ELISA assays. Cytotoxicity of H9c2 cells was quantified using the lactate dehydrogenase (LDH) cytotoxicity assay kit (cat. no. ml094790; Shanghai Enzyme-linked Biotechnology Co., Ltd.). The levels of IL-1β (cat. no. E-EL-H0149; Elabscience Bionovation Inc.), IL-6 and TNF-α (cat. nos. ml063159 and ml064303v; Shanghai Enzyme-linked Biotechnology Co., Ltd.), as well as ATP and hydrogen peroxide (H_2O_2 in H9c2 cells were analyzed by commercial assay kits (cat. nos. BC5470 and BC3590; Beijing Solarbio Science & Technology Co., Ltd.) according to the kit instructions. The levels of serum LDH, cardiac troponin I (cTn I), creatine kinase isoenzyme (CK-MB) and brain natriuretic peptide (BNP) in mice were detected by corresponding ELISA kits obtained from Shanghai Enzyme-linked Biotechnology Co., Ltd., complying with the manufacturer's instructions. The inflammatory indicators, IL-6, IL-1β and TNF-α and indicators of mitochondrial dysfunction, including ROS (ROS test kit DHE; Beijing Biolab Technology Co., Ltd.), ATP, H_2O_2 and Ca^{2+} (Screen Quest™ Luminometric Calcium Assay Kit; AAT Bioquest, Inc.), were all detected in heart tissue using the appropriate ELISA kits according to the manufacturer's instructions.

TUNEL staining. Apoptosis in H9c2 and heart tissue of mice were detected by the TUNEL assay kit (cat. no. C1090; Beyotime Biotechnology) according to the manufacturer's instruction. Briefly, heart tissue and H9c2 cells fixed in 4% PFA were treated with 50 μl prepared proteinase K working solution and TUNEL detection solution (5 μl TdT enzyme; 45 μl fluorescent labeling solution) for 1 h at 37˚C in the dark. The tissue sections or cell slides were then washed with PBS and mounted in a medium with DAPI (0.01%) for 10 min at room temperature in the dark. Afterward, 6-10 fields were randomly selected per tissue section or slide and all images were captured using the Olympus BX 53 fluorescence microscope (Olympus Corporation).

Western blotting assay. Total protein was isolated from left ventricular cardiac tissue or H9c2 cells using 1X RIPA buffer with protease cocktail inhibitor (cat. nos. P0013B and P1045; Beyotime Biotechnology). Upon quantification of protein concentration using a BCA assay, 50 μg of the samples were separated on 4-15% gels by SDS-PAGE electrophoresis. Then, the separated proteins were transferred onto PVDF membranes. After blocking the membranes with 5% skim milk at 37˚C for 1 h, they were placed in a shaking incubator at 4˚C and incubated overnight with primary antibodies. The primary antibodies used in the present study were purchased from Abcam. These included the rabbit anti-collagen I (1:1,000; ab260043), rabbit anti-collagen III (1:7,000; ab7778), rabbit anti-MMP-9 (1:1,000; ab228402), rabbit anti-cleaved caspase-3 (1:5,000; ab214430), rabbit anti-Bcl-2 (1:1,000; ab32124), rabbit anti-Bax (1:5,000; ab32503), rabbit anti-AMPK α 1 (1:2,000; ab32047), rabbit anti-AMPK α 1 (phospho-S487; 1:7,000; ab131357), rabbit anti-mTOR (1:10,000; ab134903), rabbit anti-mTOR (phospho-S2448; 1:5,000; ab109268) and rabbit anti-GAPDH (1:2,500; ab9485).

Subsequently, the membranes were incubated with the secondary antibody goat anti-rabbit IgG H&L (HRP) (1:10,000; ab6721; Abcam) at room temperature for 1 h, and protein bands were visualized by ECL kit (cat. no. P0018HS; Beyotime Biotechnology) and images captured using the Tanon 3500 chemiluminescence imaging device (Tanon Science & Technology Co., Ltd.). Band density was then examined using Image Lab Software (Bio-Rad Laboratories, Inc.).

Statistical analysis. Data are presented as mean + SD. Single two-tailed unpaired Student's t-tests were used to compare two groups and one-way ANOVA tests were used to evaluate >2 groups, with Tukey's multiple comparison tests serving as post hoc analyses. GraphPad Prism (version 9.0; Dotmatics) was used for all data analyses. $P<0.05$ was considered to indicate a statistically significant difference.

Results

SOTA ameliorates DOX-induced cardiac dysfunction and myocardial fibrosis in mice. Impacts of SOTA on the cardiac function of DOX-induced cardiomyopathy were investigated in the present study. Echocardiography was utilized to

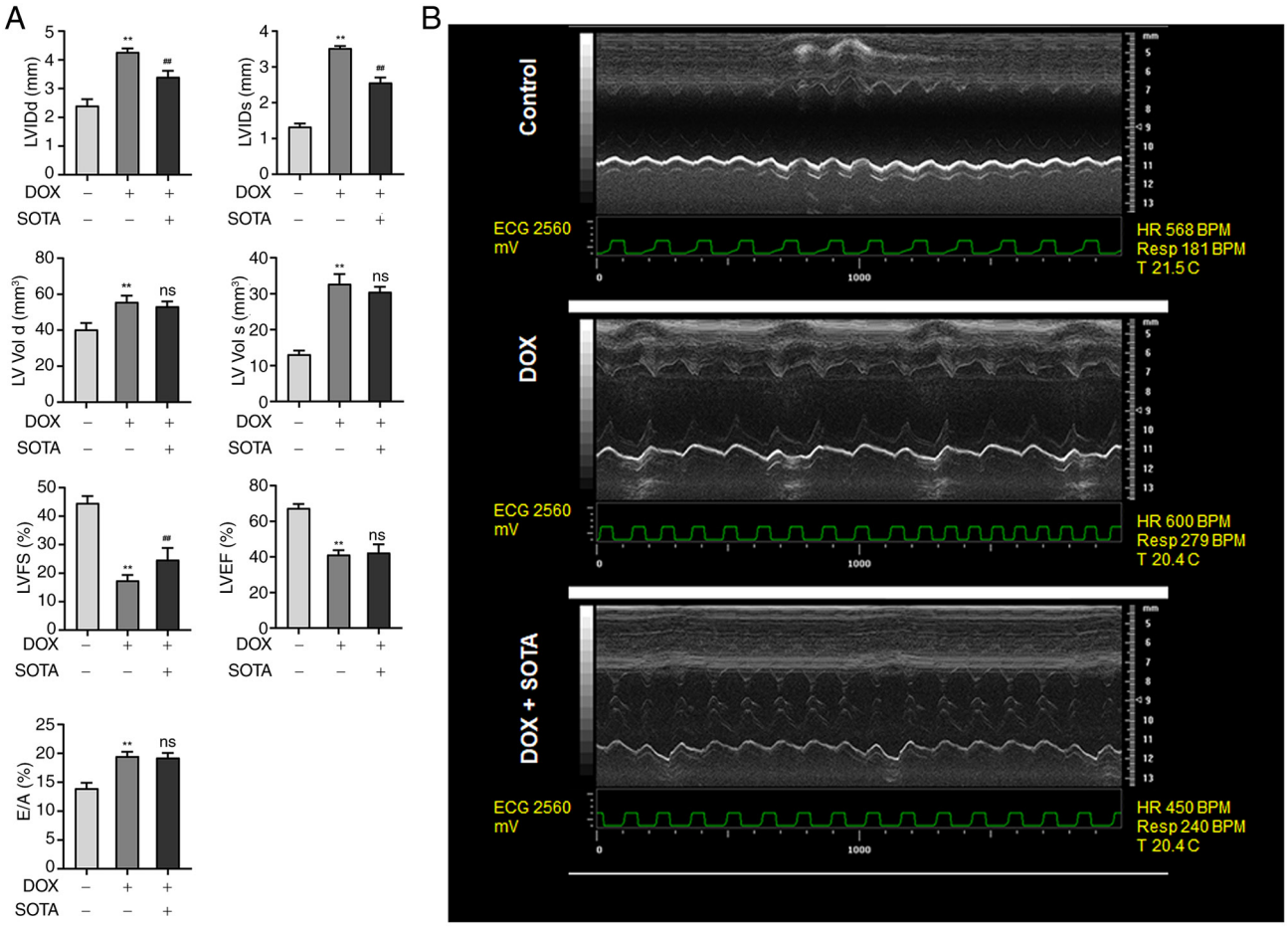

Figure 1. SOTA ameliorates DOX-induced cardiac dysfunction in mice. (A) Echocardiographic changes in cardiac function in motion-mode: LVIDd, LVIDs, LV Vol d, LV Vol s, LVFS, LVEF and E/A of mice 10 days after treatment with DOX combined with SOTA. (B) Representative echocardiogram images of mice. All data are expressed as the mean ± SD (n=6). **P<0.01 compared with the Control untreated groups and $^{\#\#}$P<0.01 compared with the DOX-alone treated group. ns, not significant; SOTA, sotagliflozin; DOX, doxorubicin; LVIDd, left ventricular internal dimensions in diastole; LVIDs, left ventricular internal dimensions in systole; LV Vol d, left ventricular volume in diastole; LV Vol s, left ventricular volume in systole; LVFS, left ventricular fractional shortening rate; LVEF, left ventricular ejection fraction; E/A, early/atrial; HR, heart rate; BPM, beats per minute; Resp, respiration rate; T, temperature; ECG, electrocardiogram.

evaluate cardiac function (Fig. 1A and B). When comparing the DOX and control groups, significant increases in LVIDd and LVIDs following DOX administration were observed, which were then notably reduced by pretreatment with SOTA (LVIDd, P<0.001; LVIDs, P<0.001). Although LV Vol d, LV Vol s and E/A were increased by DOX compared with control groups, these values were not significantly affected by exposure to SOTA (LV Vol d, P=0.48; LV Vol s, P=0.18; E/A, P=0.89). Additionally, the DOX treated group exhibited a reduction in LVFS and LVEF. Upon receiving SOTA, a partial increase in LVFS was observed. However, no increase in LVEF was detected. This suggested that DOX induced left ventricular dilated cardiomyopathy, manifested by left ventricular enlargement, diastolic dysfunction and decreased systolic function, as indicated by the decreased LVFS and LVEF. SOTA treatment partially prevented DOX-induced structural changes in the left ventricle (decreased LVIDd and LVIDs) and partially reduced systolic function impairment (as observed by the partial increase in LVFS; P=0.006), although only limited improvement in diastolic function and overall ejection fraction (LVEF) was observed (P=0.85).

Morphological changes and fibrosis of myocardial tissue were assessed using H&E and sirius red staining. H&E staining revealed that myocardial cells were orderly arranged in the control group, whereas in the DOX group, myogenic fibers were disintegrated, myocardial fibers were broken and disordered and myocardial cell spacing was increased. SOTA treatment notably improved the pathological changes (Fig. 2A). Moreover, sirius red staining showed that collagen expression was notably enhanced in the DOX group, which was diminished by the SOTA treatment (Fig. 2B). In addition, western blotting analysis revealed the upregulation of fibrosis-related proteins (collagen I, P<0.001; collagen III, P=0.02; MMP-9, P=0.03) in the DOX-treated group, which were downregulated by SOTA treatment (Fig. 2C and D). Lastly, serum levels of LDH (P<0.001) and cTn-I (P<0.001) were assessed and found to be elevated in the DOX treated group, which were attenuated by SOTA treatment. However, the DOX-upregulated CK-MB (P=0.60) and BNP (P=0.25) levels were unaffected by SOTA (Fig. 2E). Overall, these results suggested that SOTA treatment could effectively improve DOX-induced cardiac dysfunction and fibrosis in mice as observed by its effects on the levels of biomarkers of cardiomyocyte damage.

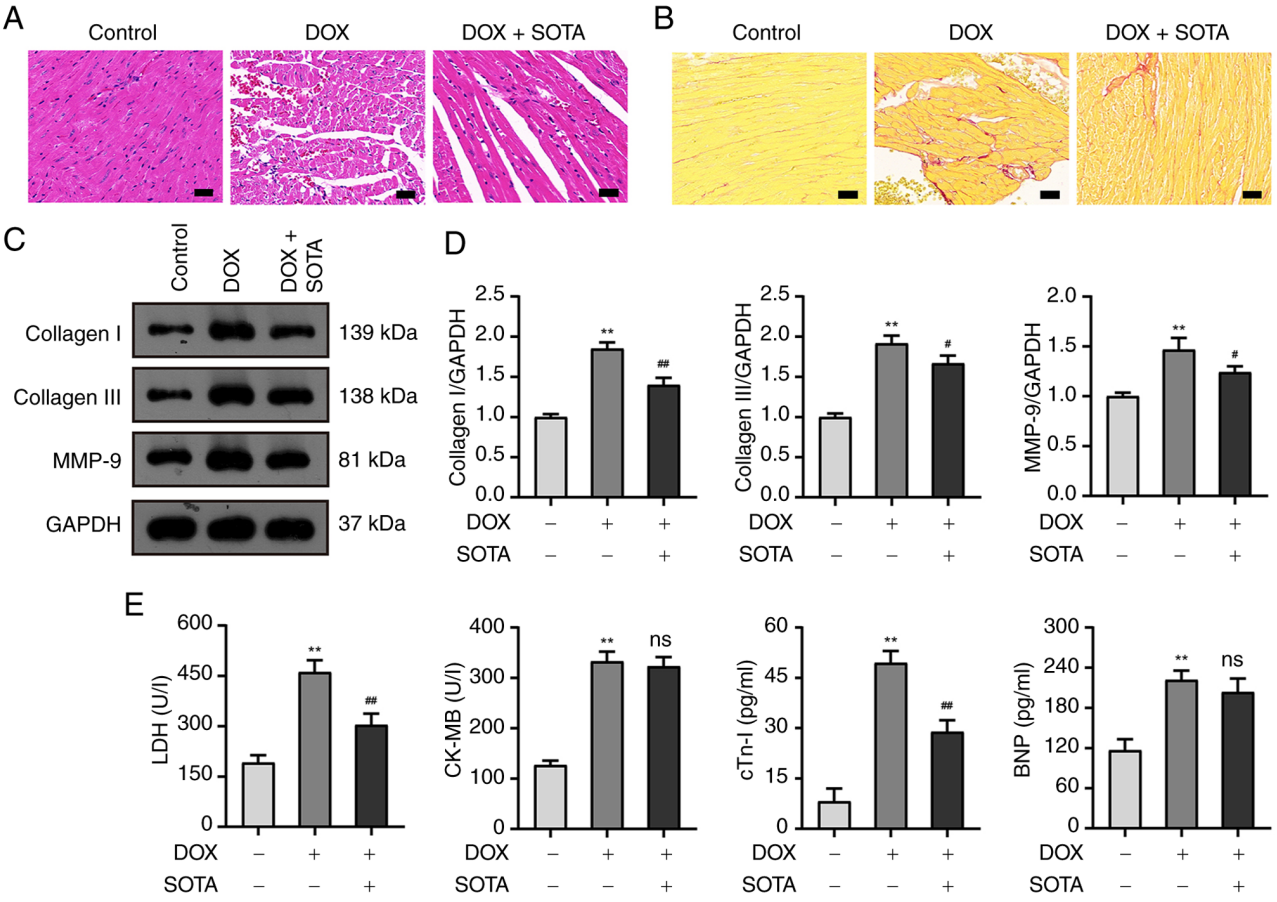

Figure 2. SOTA ameliorates DOX-induced myocardial fibrosis and morphological alteration in mice. (A) Representative images of H&E staining of heart tissues in mice. Scale bar, 20 μm. (B) Representative images of Sirius red staining of heart tissues in mice. Scale bar, 20 μm. (C) Western blotting bands and (D) semi-quantitative results of collagen I, collagen III and MMP-9 proteins of heart tissue in mice. (E) Changes in serum LDH, CK-MB, cTn-I and BNP levels were detected using commercial ELISA kits. All data are expressed as the mean ± SD (n=6). **P<0.01 compared with the Control untreated group; $^{\#}$P<0.05, $^{\#\#}$P<0.01 compared with the DOX alone group. ns, not significant; SOTA, sotagliflozin; DOX, doxorubicin; LDH, lactate dehydrogenase; CK-MB, creatine kinase isoenzyme; cTn-I, cardiac troponin I; BNP, brain natriuretic peptide; H&E, hematoxylin and eosin; MMP-9, matrix metallopeptidase 9.

SOTA attenuates DOX-induced cardiac apoptosis, inflammation and mitochondrial dysfunction in vivo. To explore the function of SOTA on DOX-induced apoptosis in the heart, a TUNEL assay was performed on the *in vivo* model. An increased rate of apoptosis was detected in the DOX-treated group but was significantly downregulated by SOTA in heart tissue (P<0.001; Fig. 3A and B). Consistently, the expression of apoptosis-related proteins cleaved caspase-3 was also increased by DOX treatment, whereas the Bcl-2/Bax ratio was decreased, which was partially prevented in heart tissue in mice (cleaved caspase-3, P=0.003; Bcl-2/Bax ratio, P<0.001) by exposure to SOTA (Fig. 3C and D). These results indicated that SOTA mitigated DOX-induced cardiac apoptosis in mice. ELISA assays revealed that the expression of IL-1β, IL-6 and TNF-α in mouse heart tissue was significantly increased following DOX administration compared with control mice, an effect inhibited by SOTA (IL-1β, P<0.001; IL-6, P<0.001; TNF-α, P<0.001), indicating that SOTA improved DOX-induced myocardial inflammation (Fig. 3E). Additional ELISA experiments showed that the levels of ROS, H_2O_2 and Ca^{2+} in mouse heart tissue increased in the DOX-treated group, whereas ATP levels decreased, but this effect was prevented with SOTA treatment (ROS, P<0.001); H_2O_2, P<0.001; Ca^{2+}, P<0.001; ATP, P=0.003; Fig. 3F), suggesting that SOTA alleviates the DOX-induced mitochondrial dysfunction in mouse heart tissue.

SOTA alleviates DOX-induced cardiotoxicity and cardiomyocyte apoptosis in vitro. To further explore the specific molecular mechanisms involved in the *in vivo* cardioprotective effects of SOTA in DOX-induced cardiotoxicity murine models, *in vitro* experiments using H9c2 cells were conducted. A previous study (5) determined that 10 μM DOX was the optimal drug concentration for the *in vitro* experiments (P<0.0001; Fig. 4A). To elucidate the mechanisms underlying SOTA effects on DOX-induced cardiotoxicity *in vitro*, H9c2 cells were treated with DOX alone or in combination with varying concentrations of SOTA (5, 10, 20 and 40 μM). The CCK-8 assay revealed that 5 μM SOTA significantly enhanced cell viability after 12 h compared with the DOX group (Fig. 4B). Therefore, a 5 μM SOTA dose and a 12 h incubation period were chosen for subsequent *in vitro* studies. LDH leakage, an indicator of cell damage, was measured in the cell culture medium. Results showed that DOX significantly increased LDH levels compared with control cells (P<0.0001), whereas DOX in combination with pretreatment of 5 μM SOTA significantly reduced the DOX-upregulated LDH levels (P=0.006; Fig. 4C).

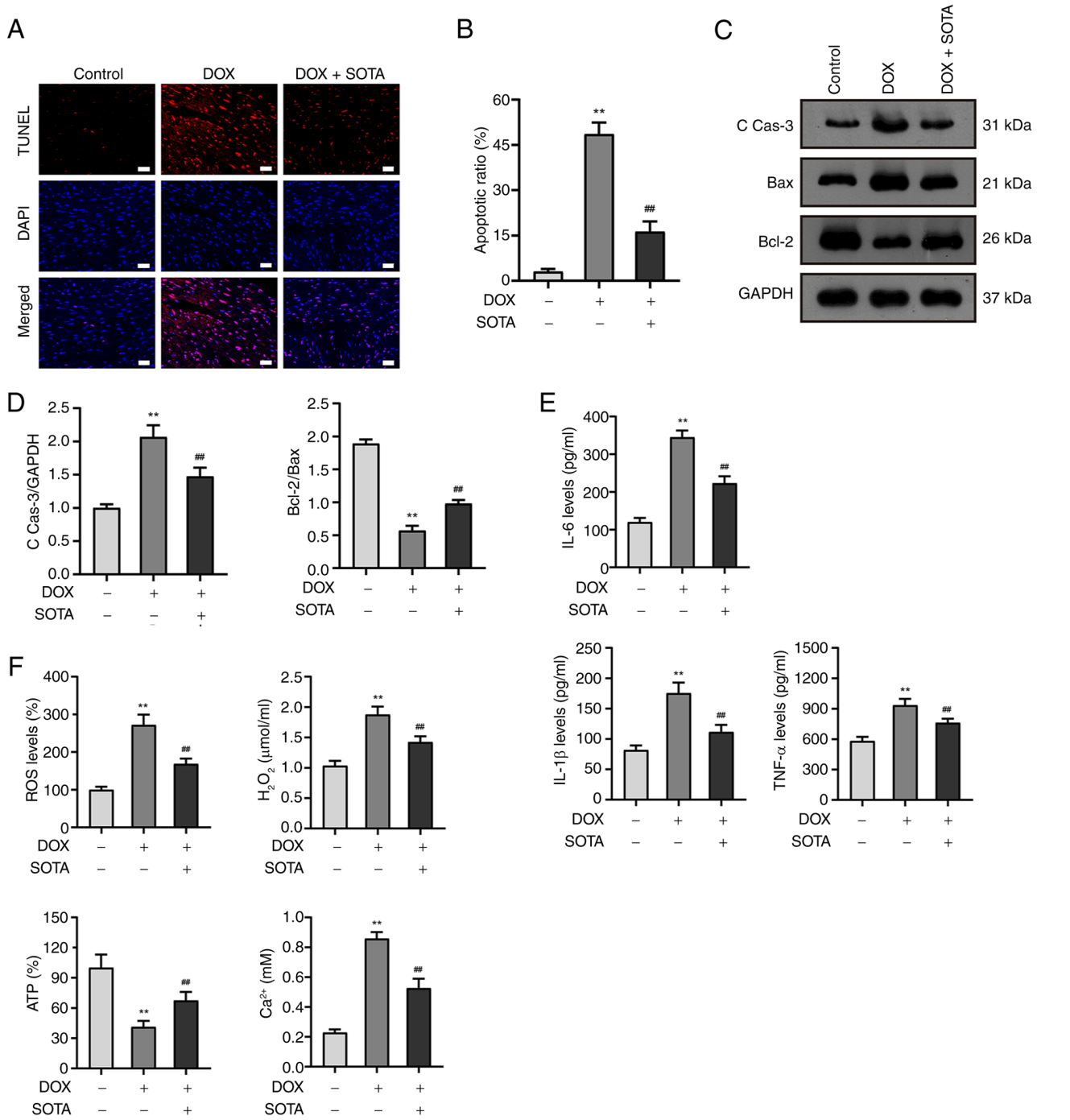

Figure 3. SOTA attenuates DOX-induced cardiac apoptosis, inflammation and mitochondrial dysfunction *in vivo*. (A) Representative images of TUNEL staining and (B) the quantitative results of heart tissue in mice. Scale bar, 20 μm. (C) Representative images of western blotting and (D) statistical results of the C cas-3, Bax and Bcl-2 proteins of heart tissue in mice. (E) The levels of IL-6, IL-1β and TNF-α in mice heart tissue as determined by commercial ELISA kits. (F) Changes in ROS, ATP, H_2O_2 and Ca^{2+} levels in mice heart tissue were detected by commercial ELISA kits. All data are expressed as the mean ± SD (n=6). **P<0.01 compared with Control untreated group, $^{\#\#}$P<0.01 compared with DOX alone group. ns, not significant; SOTA, sotagliflozin; DOX, doxorubicin; C cas-3, cleaved caspase-3; ROS, reactive oxygen species; H_2O_2, hydrogen peroxide; TUNEL, terminal deoxynucleotidyl transferase dUTP nick end labeling; DAPI, 4',6-diamidino-2-phenylindole; Bax, Bcl-2-associated X protein; Bcl-2, B-cell lymphoma 2; IL-6, interleukin-6; IL-1β, interleukin-1β; TNF-α, tumor necrosis factor-α; ATP, adenosine triphosphate; GAPDH, glyceraldehyde-3-phosphate dehydrogenase.

Consequently, SOTA can mitigate DOX-induced injury in H9c2 cells.

To investigate the impact of SOTA on DOX-induced apoptosis in the heart, a TUNEL assay was first performed *in vitro* using H9c2 cells. The DOX group had a higher rate of apoptosis, but this was significantly prevented by SOTA (P<0.001; Fig. 4D and E). Further analysis revealed that cleaved caspase-3 expression was notably increased in the DOX group, whereas the Bcl-2/Bax ratio was reduced, indicating that DOX could induce apoptosis. However, SOTA treatment significantly increased Bcl-2/Bax ratio (P<0.001) and decreased cleaved caspase-3 levels in H9c2 cells (P<0.001; Fig. 4F and G), suggesting that SOTA mitigated DOX-induced apoptosis in cardiac cells.

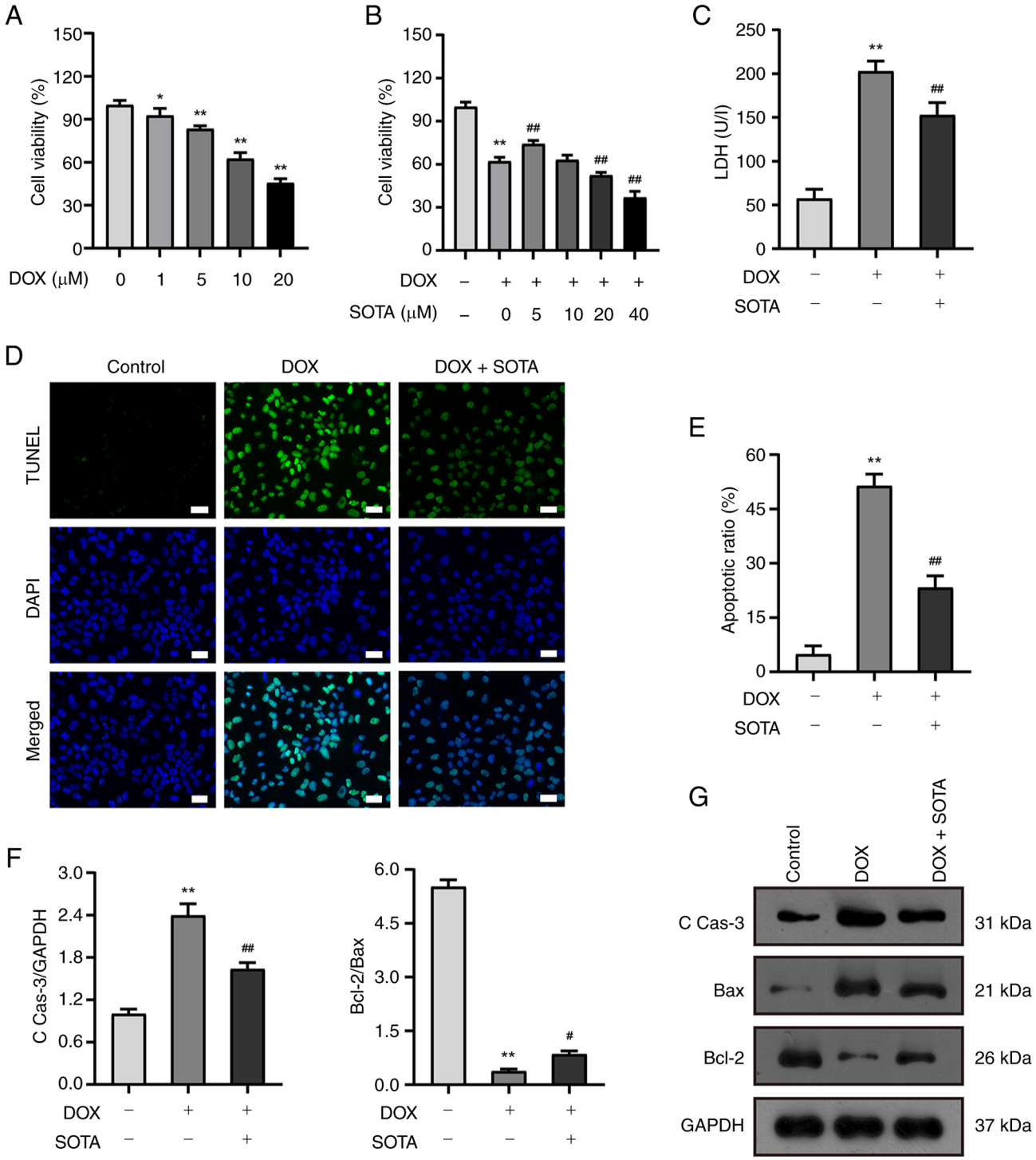

Figure 4. SOTA alleviates DOX-induced cardiotoxicity and cardiomyocyte apoptosis *in vitro*. (A) Cell viability of H9c2 cells treated with DOX (0, 5, 10, 20 and 30 μM) at 12 h. (B) Cell viability of H9c2 cells treated with DOX (10 μM) combined with SOTA (0, 5, 10, 20 and 40 μM) at 12 h. (C) LDH levels in H9c2 cells were detected by a commercial ELISA kit. (D) Representative TUNEL staining images and (E) the quantitative results of H9c2 cells. Scale bar, 20 μm. (F) Statistical results of C cas-3, Bax and Bcl-2 proteins of H9c2 cells and (G) representative images of western blotting. All data are expressed as the mean ± SD (n=3). *P<0.05, **P<0.01 compared with Control untreated groups, $^{\#}$P<0.05 and $^{\#\#}$P<0.01 compared with DOX alone group. ns, not significant; SOTA, sotagliflozin; DOX, doxorubicin; C cas-3, cleaved capsase-3; LDH, lactate dehydrogenase.

SOTA attenuates DOX-induced cardiac inflammation and mitochondrial dysfunction in vitro. To assess the efficacy of SOTA on DOX-induced inflammation in the heart, ELISA assays were first used to measure *in vitro* changes in cytokine levels in H9c2 cells. It was found that the inflammatory markers IL-6, IL-1β and TNF-α in H9c2 cells were all elevated after DOX administration (IL-6, P=0.006; IL-1β, P<0.001; TNF-α, P=0.001), but these markers were significantly reduced with SOTA administration (Fig. 5A). This suggests that SOTA may prevent DOX- induced inflammation in H9c2 cells.

Mitochondrial damage results in an elevation of ROS levels, which subsequently exacerbates mitochondrial damage (27).

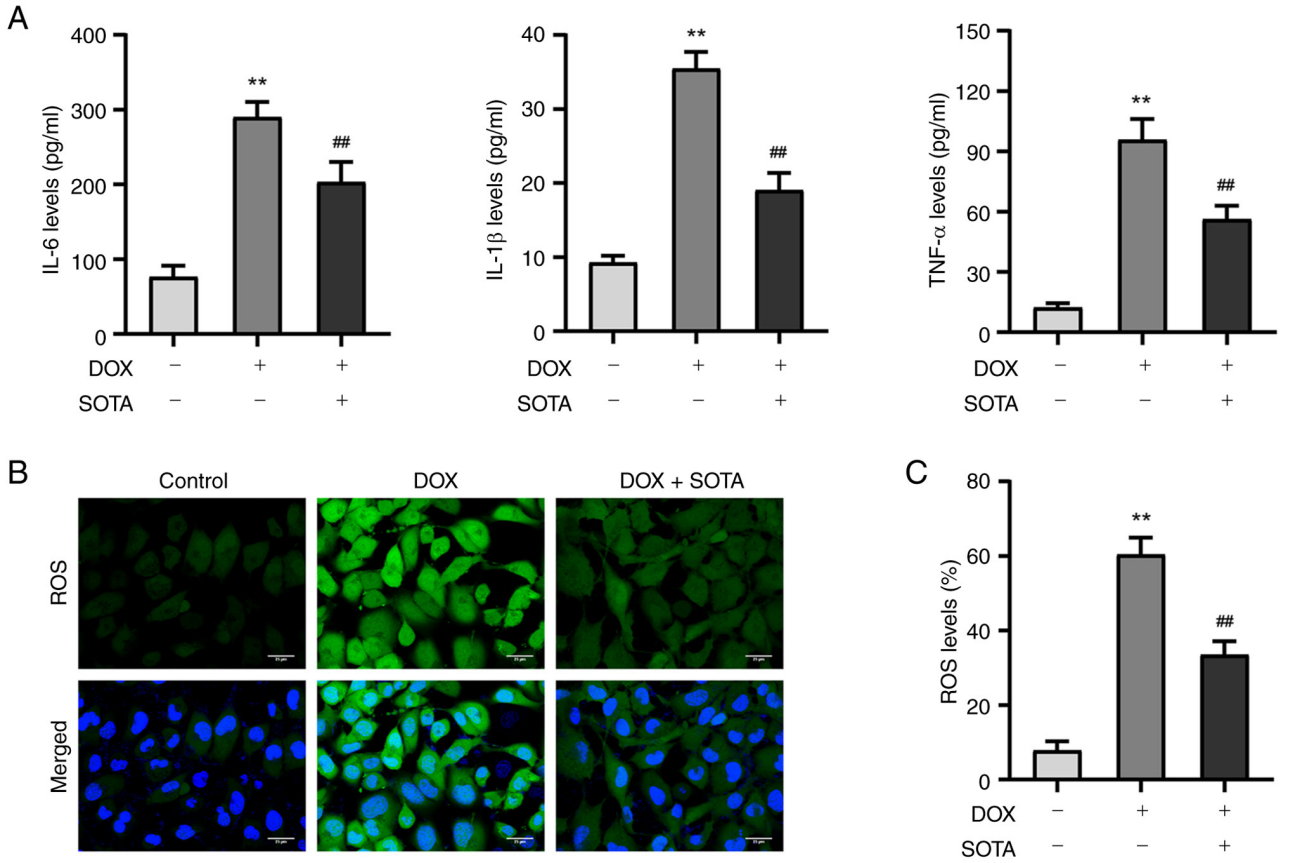

Figure 5. SOTA attenuates DOX-induced cardiac inflammation and ROS *in vitro*. (A) IL-6, IL-1β and TNF-α levels in H9c2 cells as determined by commercial ELISA kits. (B) Representative images of DCFH-DA staining and (C) the quantitative results of ROS levels in H9c2 cells. All data are expressed as the mean ± SD (n=3). Scale bar, 25 μm. **P<0.01 compared with Control untreated group; $^{\#\#}$P<0.01 compared with DOX alone group. SOTA, sotagliflozin; DOX, doxorubicin; DCFH-DA, 2',7'-dichlorodihydrofluorescein diacetate; ROS, reactive oxygen species; IL-6, interleukin-6; IL-1β, interleukin-1β; TNF-α, tumor necrosis factor-α; DAPI, 4',6-diamidino-2-phenylindole.

To investigate the efficacy of SOTA on oxidative damage in H9c2 cells activated by DOX, experiments were conducted using DCFH-DA staining, demonstrating that DOX treatment significantly increased ROS production, which was then downregulated by SOTA treatment (P<0.001; Fig. 5B and C). Simultaneously, mitochondrial damage can result in the overloading of Ca^{2+}, disruption of energy metabolism and the collapse of the MMP, thereby intensifying damage to the cardiac muscle (28). In the present study, the effects of mitochondrial Ca^{2+} overload were assessed by Rhod2-AM fluorescent probes. As shown in Fig. 6A and B, DOX significantly enhanced mitochondrial Ca^{2+} content and these changes were prevented by SOTA treatment (P<0.001). Using JC-1 staining, DOX resulted in a significant decline in the ratio of JC-1 aggregates to monomers. In healthy cells, JC-1 forms aggregates with red fluorescence, whereas in necrotic and apoptotic cells, the mitochondrial membrane potential decreases and JC-1 remains as a monomer, indicated as green fluorescence. The change in the ratio of red to green fluorescence is used as an indicator of the condition of the mitochondria. Significant attenuation of the DOX-induced mitochondrial dysfunction was observed upon exposure to SOTA (P=0.003; Fig. 6D and E). As demonstrated by the ELISA experiments, DOX significantly increased H_2O_2 levels (P=0.005) and decreased mitochondrial ATP content (P=0.03), however in both cases, results were improved by the administration of SOTA (Fig. 6C and F). Collectively, these results suggest that SOTA has the capacity to mitigate DOX-induced mitochondrial impairment in H9c2 cells.

SOTA attenuates DOX-induced cardiotoxicity by activating the AMPK/mTOR pathway in vitro. To determine the protective mechanisms of SOTA against DOX-induced cardiac injury, the potential involvement of AMPK/mTOR pathway was then examined. Notably, after the administration of DOX in H9c2 cells, phosphorylated (p)-AMPK/AMPK levels were reduced (P<0.001) and p-mTOR/mTOR was increased (P=0.010; Fig. 7A and B), yet these changes were significantly prevented by SOTA treatment (p-AMPK/AMPK, P<0.001; p-mTOR/mTOR, P<0.001; Fig. 7C and D). Furthermore, the effects of SOTA treatment were inhibited by the AMPK/mTOR pathway inhibitor compound C, a cell-permeable reversible and ATP-competitive inhibitor of AMPK increasingly used to inhibit AMPK in cell-based assays (29) (p-AMPK/AMPK, P=0.002; p-mTOR/mTOR, P<0.001; Fig. 7C and D). Overall, this evidence indicates that the AMPK/mTOR pathway can be activated by SOTA. In addition, the contribution of the AMPK/mTOR pathway to the induction of apoptosis, inflammation and mitochondrial dysfunction in H9c2 cells was also investigated. The results indicated that SOTA decreased cleaved caspase-3 levels (Fig. 7C and E), increased the Bcl-2/Bax ratio (Fig. 7C and F) and downregulated the apoptosis rate (Fig. 7G and H), which were in turn reduced by compound C

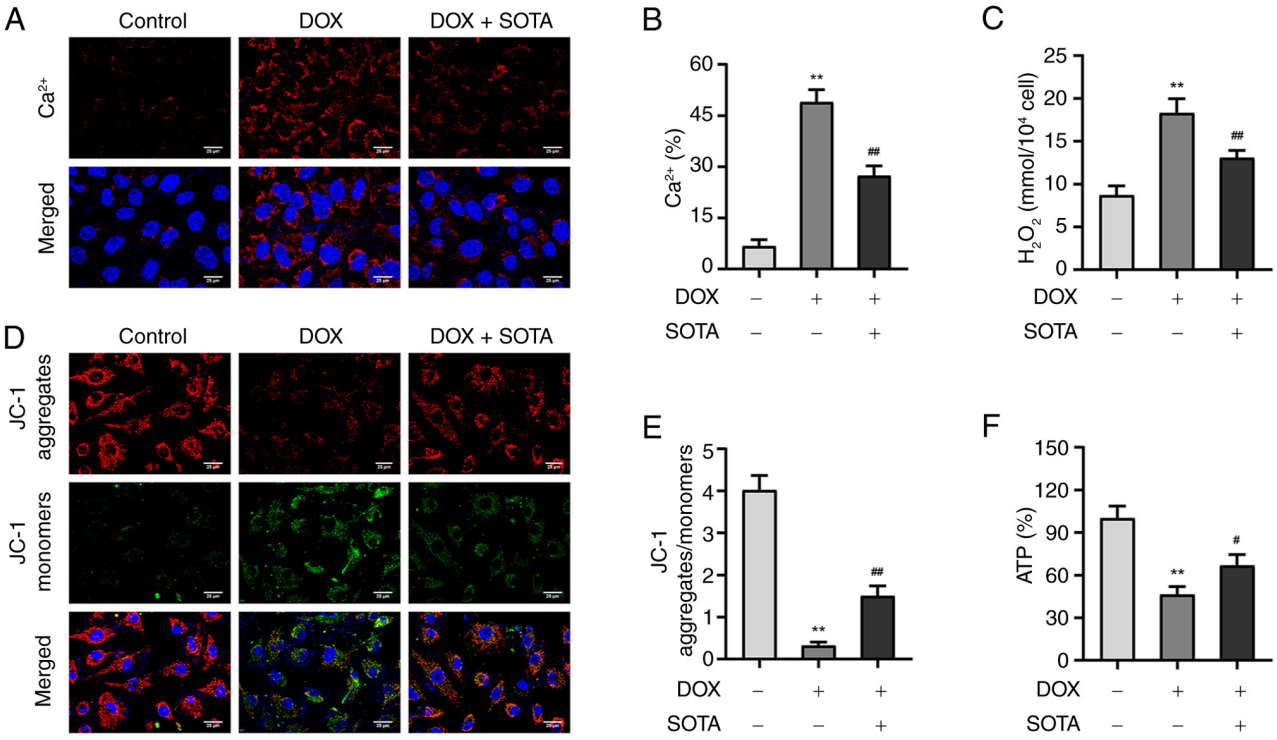

Figure 6. SOTA attenuates DOX-induced cardiac mitochondrial dysfunction *in vitro*. (A) Representative images of Rhod2-AM staining and (B) mitochondrial Ca^{2+} quantitative results in H9c2 cells. Scale bar, 25 μm. (C) H_2O_2 levels in H9c2 cells as determined by commercial ELISA kits. (D) Representative images of JC-1 staining and (E) statistical results of JC-1 aggregates to monomers in H9c2 cells. Scale bar, 25 μm. (F) ATP levels in H9c2 cells as determined by ELISA kits. All data are expressed as the mean ± SD (n=3). **P<0.01 compared with Control untreated group, $^{\#}$P<0.05 and $^{\#\#}$P<0.01 compared with DOX alone group. SOTA, sotagliflozin; DOX, doxorubicin; H2O2, hydrogen peroxide; JC-1, 5,5',6,6'-tetrachloro-1,1',3,3'-tetraethylbenzimidazolylcarbocyanine iodide; DAPI, 4',6-diamidino-2-phenylindole; ATP, adenosine triphosphate.

treatment (cleaved caspase-3, P=0.002; Bcl-2/Bax, P=0.008; apoptosis rate, P=0.008). Furthermore, SOTA decreased ROS (Fig. 8A and C) and Ca^{2+} levels (Fig. 8A and D) and upregulated JC-1 aggregates to monomers (Fig. 8B and E), which were reduced by Compound C treatment (ROS, P=0.02; Ca^{2+}, P=0.006; JC-1, P=0.003). Based on these results, SOTA could attenuate DOX-induced apoptosis and mitochondrial dysfunction by activating the AMPK/mTOR pathway in DOX-stimulated H9c2 cells, thereby reducing cardiotoxicity.

Discussion

DOX is a potent chemotherapeutic agent that can cause cardiomyopathy, a serious condition characterized by impaired cardiac function and heart failure (2). Patients diagnosed with either type 1 or type 2 diabetes and exposed to SOTA treatment exhibit a lower likelihood of cardiovascular events (12). SOTA also showed efficacy in the SOLOIST-WHF trial for the treatment of acute heart failure in patients with type 2 diabetes, who experienced fewer cardiovascular-related mortalities and heart failure-related hospitalizations (13). Thus, although the potential of SOTA in patients with heart failure has been partially studied in the context of diabetes, its specific mechanisms in DOX-induced cardiomyopathy has not been fully elucidated.

The present study investigated the cardioprotective potential of SOTA to prevent DOX-induced cardiotoxicity frequently observed during anticancer treatment of different malignancies. SOTA co-treatment attenuated DOX-induced apoptosis, inflammation, oxidative stress and mitochondrial dysfunction within *in vitro* and *in vivo* DOX-induced cardiotoxicity models by activating the AMPK/mTOR pathway. The present study provides evidence supporting SOTA as a potential agent for the treatment of DOX-induced heart failure.

SOTA is a dual inhibitor of SGLT1 and SGLT2, unlike some other medications that only target SGLT2 (30). Its potency in inhibiting SGLT2 is similar to that of other SGLT2 inhibitors, such as canagliflozin and dapagliflozin, but its potency in inhibiting SGLT1 is >10-fold higher than its predecessors (12). The efficacy of dual inhibition of both SGLT-1 and SGLT-2 also improves the activity of SOTA in mild and severe chronic kidney disease, suggesting potential further use in frail patients where therapeutic options are currently limited (12). Further, SGLT-1 and GLUT1 appear to be associated. SGLT-1 protein co-localizes with GLUT1, which is normally localized to the sarcolemma and to a lesser extent with glucose transporter 4, which can be translocated from intracellular stores to the sarcolemma when required. To the best of our knowledge, to date no inhibitor effects on cardiac SGLT1, have been demonstrated, at least at therapeutic doses (31). Insight into the function of SGLT-1 in the heart could derive from investigating the effects of phloridzin, a key dual SGLT inhibitor in animal models. A study using phloridzin, a dual SGLT inhibitor, in animal models indicated that although it does not alter baseline cardiac function, SGLT-1 inhibition during ischemia-reperfusion may enhance cardio-protection by impeding left ventricular recovery and reducing tissue ATP, glucose uptake and glycolytic activity (32). Overall,

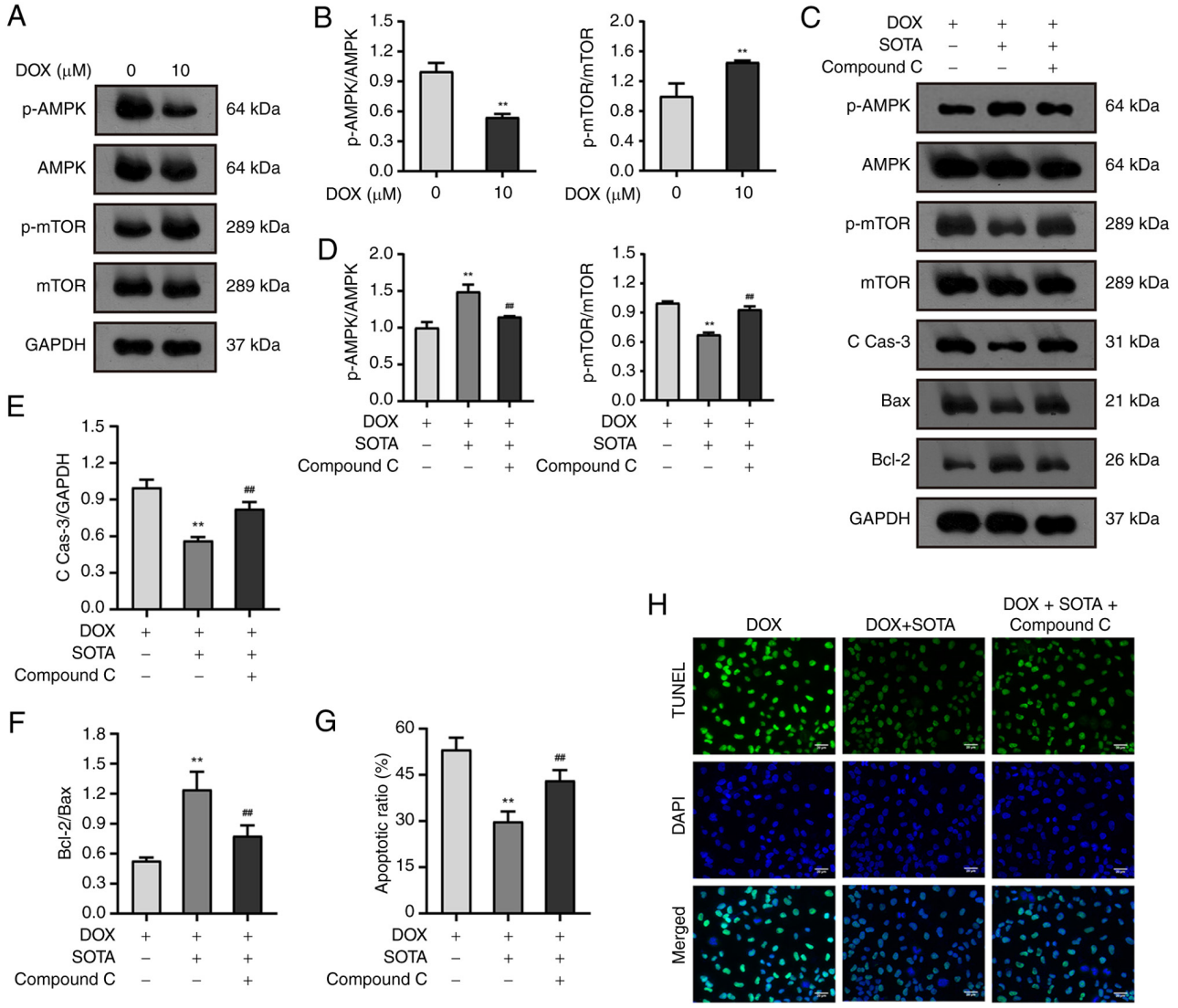

Figure 7. SOTA attenuates DOX-induced cardiomyocyte apoptosis by activating the AMPK/mTOR pathway *in vitro*. H9c2 cells were treated concomitantly with DOX and SOTA and with 10 μM of the AMPK/mTOR pathway inhibitor compound C. (A) Representative images of western blotting and (B) statistical results of p-AMPK/AMPK and p-mTOR/mTOR proteins in H9c2 cells treated with different concentrations of DOX. (C) Representative images of western blotting and (D) statistical results of p-AMPK/AMPK and p-mTOR/mTOR proteins in the presence of compound C. (E) Statistical results of C cas-3 and (F) Bcl-2/Bax proteins. (G) Quantitative results of H9c2 cells and (H) representative images of TUNEL staining. Scale bar, 20 μm. All data are expressed as the mean ± SD (n=3). *P<0.05, **P<0.01 compared with DOX group, $^{\#}$P<0.05 and $^{\#\#}$P<0.01 compared with SOTA + DOX group. SOTA, sotagliflozin; DOX, doxorubicin; p-, phosphorylated; AMPK, 5' AMP-activated protein kinase; C cas-3, cleaved caspase 3; mTOR, mechanistic target of rapamycin; Bax, Bcl-2-associated X protein; Bcl-2, B-cell lymphoma 2; TUNEL, terminal deoxynucleotidyl transferase dUTP nick end labeling; DAPI, 4',6-diamidino-2-phenylindole; GAPDH, glyceraldehyde-3-phosphate dehydrogenase.

recently completed Cardiovascular Outcome Trials, such as the SOLOIST-WHF and SCORED trials, have demonstrated that the dual inhibitor SOTA shares all the advantages of other already available SGLT-2 selective inhibitors (13,14). However, in comparison with other SGLT-2 inhibitors, the dual-inhibitor SOTA exhibits the added advantage of delaying glucose absorption in the intestine (12). This synergistic effect may positively contribute to the cardioprotective effects against DOX activity in the heart by improving the metabolic status of obese mice, reducing blood glucose, body weight and blood lipid levels. This improvement leads to a cardioprotective effect associated with the inhibition of myocardial inflammatory responses (33).

SOTA has been reported to markedly reduce the risk of cardiovascular-related mortalities and heart failure hospitalization, a benefit observed in patients with both reduced ejection fraction (HFrEF) and preserved ejection fraction (HFpEF) (13,14). To explore myocardial fibrosis as a hallmark change of cardiac remodeling and the potential clinical application of SOTA in preventing myocardial fibrosis, Young *et al* (34) evaluated transverse aortic constriction-induced myocardial hypertrophy and cardiac fibrosis in normoglycemic mice on a normal diet. The outcomes were ameliorated by SOTA treatment as observed by increasing urine output and glucose excretion. Bode *et al* (35) found SOTA improved remodeling of the left atrial associated with the metabolic syndrome rats with HFpEF, which may be associated with enhanced *in vitro* Ca^{2+}-mediated cellular arrhythmia. To the best of our knowledge, the study by Bode *et al* (35) is the first to evaluate the efficacy of SOTA,

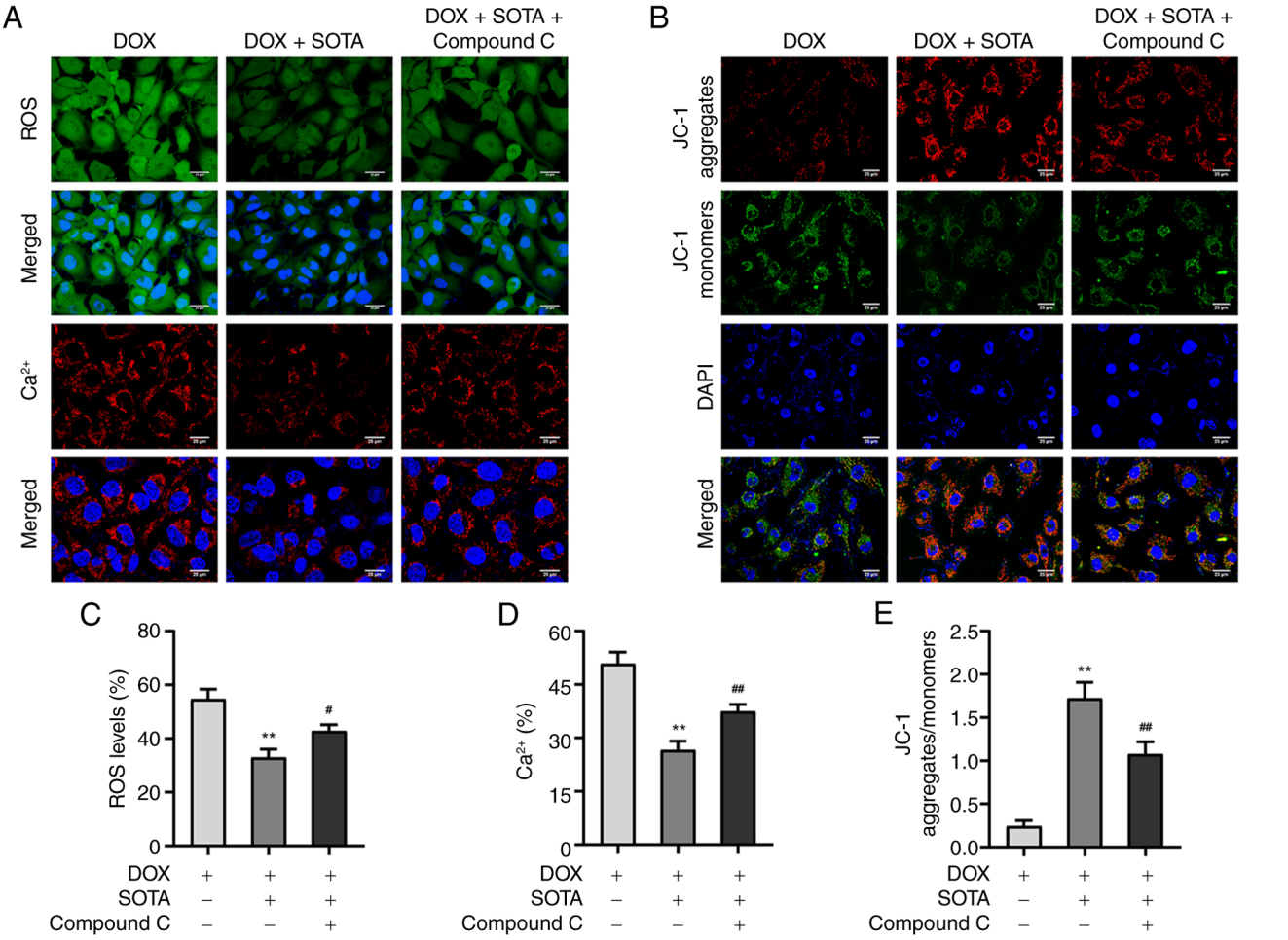

Figure 8. SOTA attenuates DOX-induced cardiac mitochondrial dysfunction by activating the AMPK/mTOR pathway *in vitro*. (A) Representative images of DCFH-DA staining and (B) representative images of JC-1 staining in H9c2 cells. (C) Quantitative results of ROS levels. (D) Quantitative mitochondrial Ca^{2+} levels in H9c2 cells. (E) Statistical results of the ratio of JC-1 aggregates to monomers. All data are expressed as the mean ± SD (n=3). **P<0.01 compared with DOX group, $^{\#}$P<0.05 and $^{\#\#}$P<0.01 compared with SOTA + DOX group. SOTA, sotagliflozin; mTOR, mechanistic target of rapamycin; DOX, doxorubicin; DCFH-DA, 2',7'-dichlorodihydrofluorescein diacetate; ROS, reactive oxygen species; JC-1, 5,5',6,6'-tetrachloro-1,1',3,3'-tetraethylbenzimidazolylcarbocyanine iodide; DAPI, 4',6-diamidino-2-phenylindole.

to alleviate heart failure. The molecular signaling pathways responsible for the cardiotoxic effects of DOX remain to be clarified, although a number of theories have been proposed, including mitochondrial dysfunction, increased ROS production, defects in iron handling and contractile failure (36-38), which are mechanisms that contribute to dilated heart disease.

In the present study, using the DOX-induced heart failure model in mice, the left ventricular systolic function, cardiac output and levels of myocardial enzymes were improved in animals treated with SOTA. Additionally, SOTA was found to alleviate myocardial fibrosis, an indicator of cardiac remodeling, as evidenced by a reduction in the expression of fibrosis-related genes and improvement in cell morphology as observed by H&E and sirius red staining. These findings suggest that SOTA can prevent cardiac remodeling during heart failure progression, at the preclinical level in non-diabetic models. However, the preventative effect of SOTA has not been demonstrated using specific indicators of cardiac function (such as LVEF), which may be related to the timeliness and intensity of different molecular mechanisms.

One important observation of the present study was that although SOTA significantly improved left ventricular structural parameters (LVIDd and LVIDs) and partial systolic function indicators (LVFS), it did not achieve statistically significant improvements in the LVEF or in the diastolic function indicator (E/A ratio) across the short 10-day intervention cycle. This limits the direct translation potential of the findings of the present study. A possible reason for this lack of improvement of LVEF and cardiac function may be attributed to the timing of the treatment intervention and its duration and may also be related to the acute and severe injury model adopted in the present study. As an established parameter for measuring overall cardiac pumping function, the recovery of the ejection fraction often relies on structural remodeling and functional compensation over time. Within the first 10 days, the efficacy of the drug may initially be reflected in preventing further expansion of the ventricle and improving contractility at the myocardial fiber level (as shown by the improvement of LVFS), whereas the improvement of the overall ejaculation fraction occurs more tardively and is a slower process. The mechanism of action of the cardioprotective effects of SOTA may involve a multistep hierarchy. The cardiac protection of SGLT1/2 inhibitors acts first on hemodynamics (reduced load) and energy metabolism. These upstream improvements may

require some time before they can eventually translate into an improvement in the macro-functional indicator of LVEF. The structural improvements observed (LVIDd/s reduction) may be considered as the first step in a functional recovery of cardiac tissue.

As aforementioned, DOX can cause cardiotoxicity leading to impaired cardiac function and heart failure. The present study found that the levels of LDH, a marker of myocardial injury, were reduced following treatment with SOTA, which indicates that cell membrane integrity was protected and SOTA mitigated DOX-induced injury. One of the mechanisms by which DOX induces cardiomyopathy is apoptosis, which is activated by caspases and DNA fragmentation. Apoptosis can be triggered by numerous factors, including oxidative stress, p53 activation, DNA damage and mitochondrial dysfunction (39). DOX generates ROS that can oxidize and damage lipids, proteins and DNA. These ROS can activate pro-apoptotic signals, including JNK, p38 and NF-kB and inhibit anti-apoptotic signals, including Bcl-2 and AKT (40,41). The present study explored the role of Bcl-2/Bax as a regulator of apoptosis and found that SOTA treatment significantly increased the Bcl-2/Bax ratio. Bcl-2 is a prototype anti-death or survival factor. Bax is a member of the Bcl-2 family and, when overexpressed, also counters the death repressor activity of Bcl-2 (42). Thus, the ratio of Bcl-2 to Bax determines cell survival or death after apoptotic stimuli induced by DOX (43). *In vitro* experiments showed that the Bcl-2/Bax ratio was decreased following DOX treatment, indicating that it could induce apoptosis, although treatment with SOTA significantly increased Bcl-2/Bax, supporting its antiapoptotic potential. Similarly, decreased cleaved caspase-3, was also reduced by SOTA treatment, which suggests that the downregulation of caspase-3 expression, a key execution enzyme in apoptosis (44), contributes to the protective effects of SOTA against DOX-included apoptosis in cardiomyocytes. DOX interacts with topoisomerase IIβ, an enzyme that regulates DNA supercoiling and transcription to inhibit its activity and induce double-strand breaks in DNA. This activates the DNA damage response, p53 action and finally, induces apoptosis (45). The results of the present study suggested that SOTA administration reduces the proportion of apoptotic cells both in H9c2 cells and in mice, an effect accompanied by alterations in apoptosis-related proteins, thus indicating the potential of SOTA to suppress cardiomyocyte apoptosis in DOX-induced cardiomyopathy.

An additional mechanism involved in DOX cardiomyopathy is inflammation, which contributes to oxidative damage, mitochondrial dysfunction and myocyte cell death. DOX induces the expression of several inflammatory mediators in cardiac cells, such as IL-6, TNF-α and TLR4. These mediators activate downstream signaling pathways that promote inflammation, fibrosis and apoptosis (9,46,47). In addition, DOX activates the NLRP3 inflammasome, which cleaves IL-1β and IL-18 into their active forms. NLRP3 also triggers pyroptosis, a form of regulated cell death that releases inflammatory contents into the extracellular space (48,49). Therefore, inflammation is key in the pathogenesis of DOX-induced cardiomyopathy and presents a potential target for therapeutic intervention.

SOTA appears to alleviate cardiac damage by activating the TLR4/CaMKII pathway (22) and by ameliorating Ang II-induced oxidative stress and senescence, which in turn improve coronary artery endothelial dysfunction through the Ang II type 1 receptor/NADPH oxidase pathways (23). SOTA also attenuates ROS generation and inflammatory cytokine production in coronary endothelial cells, contributing to the reduction of atherosclerotic thrombosis (24,25). Furthermore, the present study demonstrated that SOTA administration reduced the levels of cardiac inflammatory mediators, namely IL-1, IL-6 and TNF-α. Therefore, SOTA may represent a novel interventional agent for inflammation induced by DOX in cardiomyopathy.

Mitochondria serve a key role in cardiomyocyte energy metabolism. One of the mechanisms of DOX cardiomyopathy is mitochondrial dysfunction, which involves oxidative damage, impaired oxidative phosphorylation, mitochondrial DNA (mtDNA) damage and permeability transition (28). A number of studies have shown that DOX induces mtDNA mutations, deletions and depletion in human and animal hearts, leading to reduced mitochondrial function and ATP production (50,51). Moreover, DOX causes lipid peroxidation, which damages mitochondrial DNA and proteins, further impairing the mitochondrial functions responsible for energy production and cellular homeostasis. Oxidative stress can trigger the opening of more mitochondrial permeability transition pores. This leads to an increase in MMP distribution and induces its morphological changes (52). These mitochondrial alterations may contribute to cardiomyopathy by triggering apoptotic and necrotic cell death pathways, disrupting calcium homeostasis and impairing autophagy and mitophagy processes (53,54). In accordance with prior research, the present study found that DOX-induced cardiac oxidative stress and led to elevated MMP and calcium homeostasis imbalance (6,9,11,24,39,45,50,54), which was reduced upon exposure to SOTA. Therefore, given the notable role of mitochondrial dysfunction in DOX-induced cardiomyopathy, SOTA may contribute to a novel therapeutic strategy to control this complication.

The AMPK/mTOR pathway serves a key role in regulating energy homeostasis and cellular metabolism in the heart. AMPK functions as an energy sensor, promoting catabolic processes including fatty acid oxidation and autophagy while inhibiting anabolic methods for protein and lipid synthesis. mTOR is a nutrient sensor that activates protein synthesis, cell proliferation and mitochondrial biogenesis. The AMPK/mTOR pathway is key in preserving cardiac function and responding to various stressors, including exercise, ischemia, hypertrophy and heart failure.

Dysregulation of the AMPK/mTOR pathway is associated with the progression of cardiac aging and heart failure, characterized by impaired cardiac contractility, fibrosis, inflammation, oxidative stress and mitochondrial dysfunction (55-57). By contrast, activation of the AMPK/mTOR pathway can prevent mitochondrial dysfunction and myocyte apoptosis, thereby mitigating myocardial ischemia-reperfusion injury and notably reducing the myocardial infarct area (58). DOX induces the overproduction of ROS that damages mitochondria and DNA. This leads to an imbalance in energy homeostasis and to the disruption of autophagic flux. DOX can inhibit AMPK activation and/or activate mTOR, which suppresses autophagy and

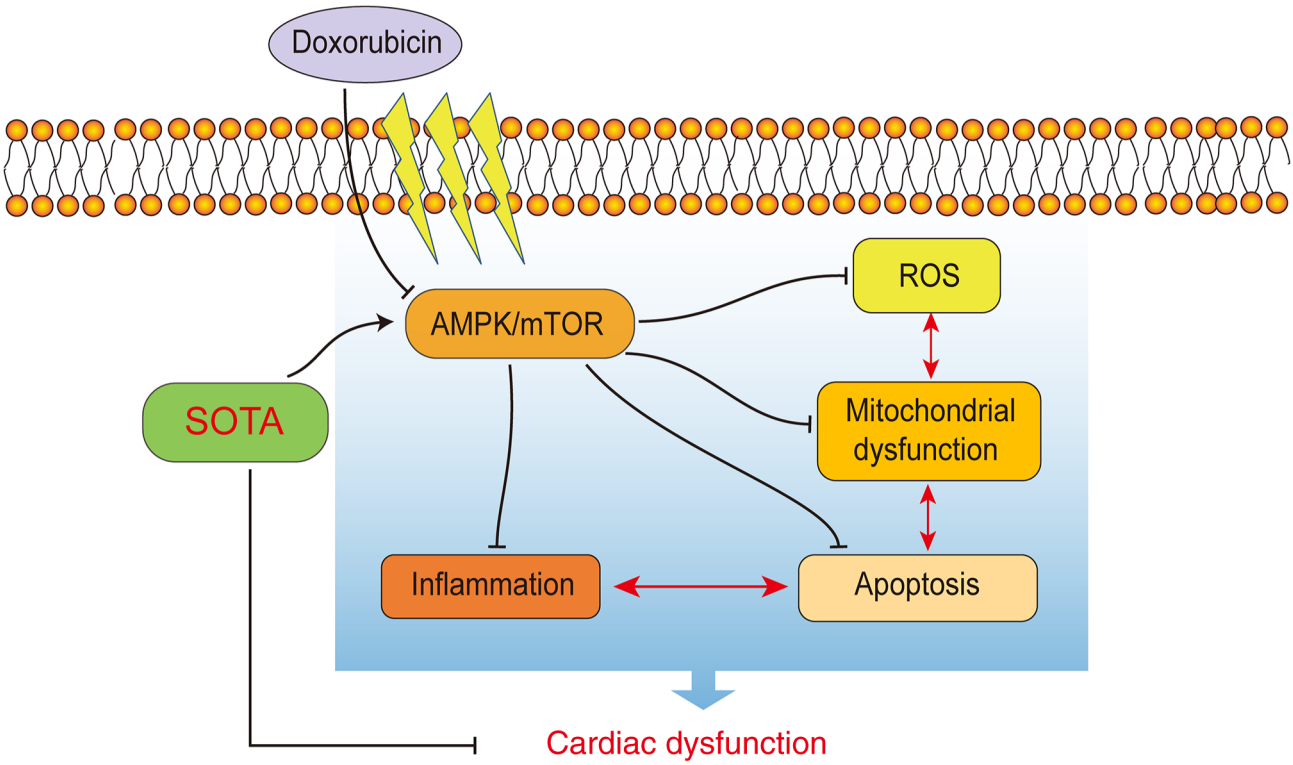

Figure 9. Schematic diagram showing protective signaling of SOTA on doxorubicin-induced cardiomyopathy. SOTA, sotagliflozin; AMPK, 5' AMP-activated protein kinase; ROS, reactive oxygen species; mTOR, mechanistic target of rapamycin.

prevents the removal of damaged mitochondria and proteins, leading to oxidative damage and apoptosis (59,60). Previous research has demonstrated that pharmacological agents that activate AMPK or inhibit mTOR, such as metformin or rapamycin, can enhance autophagy and reduce oxidative stress, mitochondrial impairment and apoptosis in DOX-injured cardiomyocytes, thus exerting cardioprotective effects (61). In the present study, SOTA activated AMPK, inhibited mTOR and attenuated cardiomyocyte apoptosis, oxidative stress and mitochondrial dysfunction, including calcium homeostasis and elevated mitochondrial membrane potential, through the AMPK/mTOR pathway. When AMPK inhibitor compound C was applied, the protective effects of SOTA against DOX cardiomyopathy were notably reduced, further demonstrating that SOTA activated the AMPK/mTOR pathway to inhibit DOX-induced impairment. Overall, these findings highlight the association between the AMPK/mTOR pathway and apoptosis, inflammation and mitochondrial function. Inhibition of AMPK activity by exposure to compound C reduced the protective effects of SOTA, which reinforces the central role of the AMPK/mTOR pathway in this mechanism. AMPK activation controls numerous cellular processes and, in the heart, it serves a key role in preventing the onset and progression of heart failure by limiting ROS levels and can prevent both HFpEF and HFrE (62). Furthermore, AMPK activation is a key component of the adaptive response to cardiomyocyte stress that occurs during myocardial ischemia. AMPK activation may prime organs and tissues for protection against ischemic injury and the early resolution of inflammation, thus representing an important druggable target for a number of diseases, including inflammation, ischemia, diabetes, obesity and aging (63).

The role of AMPK in the heart is complex and multifaceted. Although it serves a key role in the adaptive response to stress and can exhibit pleiotropic cardioprotective effects, AMPK signaling can also contribute to pathological processes such as cardiac hypertrophy and serve a key role in the progression of heart failure. Acting as a central energy sensor, AMPK enhances cardiac function by optimizing energy supply; it mitigates heart failure progression by regulating critical intracellular physiological processes, such as ATP biosynthesis and mitochondrial biogenesis, thereby delaying myocardial fibrosis and alleviating cardiac injury (64). Nrf2, downstream of AMPK, contributes to the protective effects exhibited by AMPK. Nrf2, a transcription factor, is important in mitigating oxidative stress and inflammation. With this, AMPK can activate Nrf2 to enhance its protective functions in other organ systems such as the lung (65) and in conditions such as obesity (66). In acute lung injury, AMPK induces the dissociation of Nrf2 from kelch-like ECH-associated protein-1 and facilitates its translocation into the nucleus to trigger the transcription of downstream antioxidant genes, ultimately suppressing the expression of inflammatory cells in the lungs (65). Furthermore, an interaction between Nrf2 and AMPK has been observed in a previous study using xanthohumol (XN) as an activator of both the AMPK and the Nrf2 signaling pathway (67). AMPK also activates Nrf2/heme oxygenase 1 (HO-1) signaling in mouse embryonic fibroblasts. Genetic ablation and pharmacological inhibition of AMPK interferewith Nrf2-dependent HO-1 expression by XN at the mRNA level. In turn, exposure to XN leads to AMPK activation through interference with mitochondrial function and activation of liver kinase B1 as

an upstream AMPK kinase (67). Thus, tight cooperation between signaling pathways controls cellular redox, energy or protein homeostasis.

In patients with obesity, bariatric surgery indirectly regulates the expression of downstream targets such as SIRT1, protein kinase C-ζ and nuclear receptor subfamily 4 group A member 1 by activating the AMPK pathway (68,69). This activation can lead to enhanced fatty acid oxidation, improved glucose metabolism and increased mitochondrial function. Bariatric surgery enhances the phosphorylation of AMPK and Nrf2, facilitating the binding of Nrf2 to the ABCG2 promoter region to exert renoprotective effects. Given their diverse roles, AMPK and Nrf2 demonstrate promise as novel treatment targets for acute lung injury and may also potentially contribute to reducing acute injury to the heart. Understanding the intricate mechanisms of AMPK regulation and its diverse effects is key in developing effective strategies to harness its therapeutic potential in cardiovascular disease.

At present, direct data on the interaction of SOTA on the anti-tumor activity of DOX are still limited. However, studies evaluating other SGLT2 inhibitors (such as empagliflozin and canagliflozin) provide some insight. For example, a number of preclinical studies have shown that SGLT2 inhibitors do not weaken the killing effect of DOX in cell lines such as breast cancer and liver cancer, but may even produce a synergistic anti-cancer effect with chemotherapy drugs by regulating the energy metabolism of tumor cells (inhibition of glycolysis) (70,71). Another study reported that empagliflozin does not affect the pro-apoptotic effect of DOX on breast cancer cells, but may enhance DOX-induced cytotoxicity *in vitro*, providing support for its combination with DOX in cancer therapy (72). In addition, an *in vitro* study has shown that combining DOX and empagliflozin in the treatment of triple-negative breast cancer can reduce the effective dose of DOX and may reduce its toxic side effects (especially cardiotoxicity) and chemoresistance (73).

Despite this, these findings cannot be directly equated with the anticancer effects of SOTA. Given that the dual inhibition of SGLT1 and SGLT2 may have different effects on the energy supply of specific types of cancer, such as intestinal tumors, future studies must be conducted to evaluate the specific anticancer efficacy and safety of SOTA when used in combination with DOX in different cancer models. Thus, it is advisable to exercise caution when considering the application of SOTA to clinical oncology treatment in the absence of conclusive evidence.

A key consideration in the present study design is the 10-day administration period for SOTA, which warrants discussion. While the clinical benefits of some cardiovascular drugs in chronic conditions may only become apparent after prolonged treatment, the present study utilized a DOX-induced acute cardiotoxicity model. This model is characterized by a rapid and severe pathological progression, unlike the slow development of chronic heart failure. It is an established model in cardiomyopathy research for observing acute myocardial injury and evaluating the efficacy of short-term therapeutic interventions (74,75).

Finally, a number of important limitations to the present study should be acknowledged. First, the SOLOIST-WHF and SCORED trials demonstrated that SOTA reduced cardiovascular mortality and heart failure-related hospitalizations in patients with diabetes (13,14). The present study found that SOTA improved heart failure in a non-diabetic model at the cellular and preclinical levels. However, to verify the effect of SOTA in individuals with heart failure without diabetes, dedicated clinical trials are warranted. Second, the most studied SGLT2 inhibitors are canagliflozin, dapagliflozin and empagliflozin. Future studies should compare SOTA with these agents, aiming to determine the differential value of various SGLT2 inhibitors during DOX treatment. Third, using only H9c2 cells as the *in vitro* model may limit the generalizability of the present findings as these cells do not fully replicate the responses of adult cardiomyocytes. H9c2 cells, although often used as a model for cardiomyocytes, exhibit numerous key differences from their adult counterparts. Primarily, the H9c2 cell line is derived from embryonic rat ventricles. H9c2 cells are considered cardiomyoblasts, meaning they are immature cells, whereas adult cardiomyocytes are fully differentiated and functional muscle cells. Furthermore, H9c2 cells lack spontaneous contractile properties in culture-like primary neonatal cardiomyocytes and lack the mature sarcomeric organization of adult cells. Furthermore, these cells also exhibit a different gene expression profile, particularly in regard to sarcomeric proteins and calcium handling machinery. Thus, their limitations should be considered when interpreting results and extrapolating to an *in vivo* context. Finally, the present study failed to directly observe the morphological changes of mitochondria through transmission electron microscopy. Fourth, regarding the assessment of apoptotic signaling, this study evaluated the expression of cleaved caspase-3 normalized to the internal control (GAPDH) to indicate the activation of apoptosis. The levels of total caspase-3 were not detected, and therefore, the ratio of cleaved caspase-3 to total caspase-3 was not determined. While cleaved caspase-3 is the functional executioner of apoptosis, the present study acknowledges the absence of total caspase-3 data as a limitation of this study. Future research should aim to include transmission electron microscopy technology to more intuitively verify the protective effect of SOTA on the mitochondrial ultrastructure.

In conclusion, the present study found that SOTA protects the heart from DOX-induced cardiomyopathy by modulating the AMPK/mTOR signaling pathway, thereby attenuating apoptosis, inflammation and mitochondrial dysfunction. Fig. 9 summarizes the potential cardioprotective mechanisms induced by SOTA in DOX-induced cardiopathy. SOTA activates the AMPK/mTOR signaling pathway with positive effects on cardiomyocyte apoptosis via changes in the Bcl2/Bax ratio and cleaved caspase-3 generation, oxidative stress induced by ROS and mitochondrial dysfunction, including calcium homeostasis and elevated mitochondrial membrane potential, mechanisms that contribute to enhance cardiomyocyte viability during heart failure. The present study elucidates partial cardioprotective mechanisms of SOTA and provides further evidence for SOTA treatment of heart failure. Additional studies are needed to evaluate the cardioprotective effects of SOTA in combination with DOX treatment.

Acknowledgements

Not applicable.

Funding

The present study was supported by the Supported by Fujian Provincial Natural Science Foundation Program (grant no. 2025J01152) and The Doctoral Seedling Project of the Second Affiliated Hospital of Fujian Medical University (grant no. BS202403) as well as the Health and Hygiene Appropriate Technology Project of National Health Commission's Medical and Health Science and Technology Development Research Center (grant no. 80).

Availability of data and materials

The data generated in the present study may be requested from the corresponding author.

Authors' contributions

HL and ML designed and performed the main research. DH analyzed the data and prepared the figures. ML wrote the manuscript and HL critically reviewed and revised the paper. HL and ML confirm the authenticity of all the raw data. All authors have read and approved the final version of the manuscript.

Ethics approval and consent to participate

The Animal Experimental Research Ethics Committee at Fujian Medical University (Fujian, China) approved the present study (approval no. 599).

Patient consent for publication

Not applicable.

Competing interests

The authors declare that they have no competing interests.

References

1. Khalili-Tanha G and Moghbeli M: Long non-coding RNAs as the critical regulators of doxorubicin resistance in tumor cells. Cell Mol Biol Lett 26: 39, 2021.
2. Takemura G and Fujiwara H: Doxorubicin-induced cardiomyopathy from the cardiotoxic mechanisms to management. Prog Cardiovasc Dis 49: 330-352, 2007.
3. Shabalala S, Muller CJF, Louw J and Johnson R: Polyphenols, autophagy and doxorubicin-induced cardiotoxicity. Life Sci 180: 160-170, 2017.
4. Quagliariello V, De Laurentiis M, Rea D, Barbieri A, Monti MG, Carbone A, Paccone A, Altucci L, Conte M, Canale ML, *et al*: The SGLT-2 inhibitor empagliflozin improves myocardial strain, reduces cardiac fibrosis and pro-inflammatory cytokines in non-diabetic mice treated with doxorubicin. Cardiovasc Diabetol 20: 150, 2021.
5. Rea D, Coppola C, Barbieri A, Monti MG, Misso G, Palma G, Bimonte S, Zarone MR, Luciano A, Liccardo D, *et al*: Strain analysis in the assessment of a mouse model of cardiotoxicity due to chemotherapy: Sample for preclinical research. In Vivo 30: 279-290, 2016.
6. Jiang Y and Zhang Q: Catalpol ameliorates doxorubicin-induced inflammation and oxidative stress in H9C2 cells through PPAR-γ activation. Exp Ther Med 20: 1003-1011, 2020.
7. Aryal B and Rao VA: Deficiency in cardiolipin reduces doxorubicin-induced oxidative stress and mitochondrial damage in human B-lymphocytes. PLoS One 11: e0158376, 2016.
8. Gorini S, De Angelis A, Berrino L, Malara N, Rosano G and Ferraro E: Chemotherapeutic drugs and mitochondrial dysfunction: Focus on doxorubicin, trastuzumab and sunitinib. Oxid Med Cell Longev 2018: 7582730, 2018.
9. Shi S, Chen Y, Luo Z, Nie G and Dai Y: Role of oxidative stress and inflammation-related signaling pathways in doxorubicin-induced cardiomyopathy. Cell Commun Signal 21: 61, 2023.
10. Liu Y, Chen L, Wu H and Zhang H: Delivery of astragalus polysaccharide by ultrasound microbubbles attenuate doxorubicin-induced cardiomyopathy in rodent animals. Bioengineered 13: 8419-8431, 2022.
11. Babaei-Kouchaki S, Babapour V, Panahi N and Badalzadeh R: Effect of troxerutin on oxidative stress and expression of genes regulating mitochondrial biogenesis in doxorubicin-induced myocardial injury in rats. Naunyn Schmiedebergs Arch Pharmacol 393: 1187-1195, 2020.
12. Cefalo CMA, Cinti F, Moffa S, Impronta F, Sorice GP, Mezza T, Pontecorvi A and Giaccari A: Sotagliflozin, the first dual SGLT inhibitor: Current outlook and perspectives. Cardiovasc Diabetol 18: 20, 2019.
13. Bhatt DL, Szarek M, Steg PG, Cannon CP, Leiter LA, McGuire DK, Lewis JB, Riddle MC, Voors AA, Metra M, *et al*: Sotagliflozin in patients with diabetes and recent worsening heart failure. N Engl J Med 384: 117-128, 2021.
14. Bhatt DL, Szarek M, Pitt B, Cannon CP, Leiter LA, McGuire DK, Lewis JB, Riddle MC, Inzucchi SE, Kosiborod MN, *et al*: Sotagliflozin in patients with diabetes and chronic kidney disease. N Engl J Med 384: 129-139, 2021.
15. Chen Y and Peng D: New insights into the molecular mechanisms of SGLT2 inhibitors on ventricular remodeling. Int Immunopharmacol 118: 110072, 2023.
16. Cowie MR and Fisher M: SGLT2 inhibitors: Mechanisms of cardiovascular benefit beyond glycaemic control. Nat Rev Cardiol 17: 761-772, 2020.
17. Dabour MS, George MY, Daniel MR, Blaes AH and Zordoky BN: The cardioprotective and anticancer effects of SGLT2 inhibitors: JACC: CardioOncology state-of-the-art review. JACC CardioOncol 6: 159-182, 2024.
18. Ferrannini E: Sodium-glucose co-transporters and their inhibition: Clinical physiology. Cell Metab 26: 27-38, 2017.
19. La Grotta R, Frigé C, Matacchione G, Olivieri F, de Candia P, Ceriello A and Prattichizzo F: Repurposing SGLT-2 inhibitors to target aging: Available evidence and molecular mechanisms. Int J Mol Sci 23: 12325, 2022.
20. Packer M: Role of deranged energy deprivation signaling in the pathogenesis of cardiac and renal disease in states of perceived nutrient overabundance. Circulation 141: 2095-2105, 2020.
21. Ren D, Sun Y, Zhang D, Li D, Liu Z, Jin X and Wu H: SGLT2 promotes pancreatic cancer progression by activating the Hippo signaling pathway via the hnRNPK-YAP1 axis. Cancer Lett 519: 277-288, 2021.
22. Gong Y, Kong B, Shuai W, Chen T, Zhang J and Huang H: Effect of sotagliflozin on ventricular arrhythmias in mice with myocardial infraction. Eur J Pharmacol 936: 175357, 2022.
23. Park SH, Belcastro E, Hasan H, Matsushita K, Marchandot B, Abbas M, Toti F, Auger C, Jesel L, Ohlmann P, *et al*: Angiotensin II-induced upregulation of SGLT1 and 2 contributes to human microparticle-stimulated endothelial senescence and dysfunction: Protective effect of gliflozins. Cardiovasc Diabetol 20: 65, 2021.
24. Sherratt S, Libby P, Bhatt DL and Mason P: Abstract 13422: Sotagliflozin, a dual SGLT-1/2 inhibitor, modulated expression of endothelial proteins that inhibit reactive oxygen species during inflammation compared with empagliflozin. Circulation 146 (Suppl 1): A13422, 2022.
25. Sherratt SCR, Libby P, Bhatt DL and Mason RP: Sotagliflozin, a dual SGLT 1 and 2 inhibitor, modulated expression of atheroprotective proteins during inflammation compared with empagliflozin. J Am Coll Cardiol 81 (8 Suppl): S2038, 2023.
26. National Research Council (US) Institute for Laboratory Animal Research. Guidance for the description of animal research in scientific publications. Washington (DC): National Academies Press (US), 2011.
27. Wallace KB, Sardão VA and Oliveira PJ: Mitochondrial determinants of doxorubicin-induced cardiomyopathy. Circ Res 126: 926-941, 2020.
28. Li Y, Ma Y, Dang QY, Fan XR, Han CT, Xu SZ and Li PY: Assessment of mitochondrial dysfunction and implications in cardiovascular disorders. Life Sci 306: 120834, 2022.

29. Zhou G, Myers R, Li Y, Chen Y, Shen X, Fenyk-Melody J, Wu M, Ventre J, Doebber T, Fujii N, *et al*: Role of AMP-activated protein kinase in mechanism of metformin action. J Clin Invest 108: 1167-1174, 2001.
30. Lapuerta P, Zambrowicz B, Strumph P and Sands A: Development of sotagliflozin, a dual sodium-dependent glucose transporter 1/2 inhibitor. Diab Vasc Dis Res 12: 101-110, 2015.
31. Zambrowicz B, Freiman J, Brown PM, Frazier KS, Turnage A, Bronner J, Ruff D, Shadoan M, Banks P, Mseeh F, *et al*: LX4211, a dual SGLT1/SGLT2 inhibitor, improved glycemic control in patients with type 2 diabetes in a randomized, placebo-controlled trial. Clin Pharmacol Ther 92: 158-169, 2012.
32. Kashiwagi Y, Nagoshi T, Yoshino T, Tanaka TD, Ito K, Harada T, Takahashi H, Ikegami M, Anzawa R and Yoshimura M: Expression of SGLT1 in human hearts and impairment of cardiac glucose uptake by phlorizin during ischemia-reperfusion injury in mice. PLoS One 10: e0130605, 2015.
33. Luo JC, Jin LH, Zhong YS, Xu XY, Zhang ZY, Chen J, Chen ZX, Li S, Zhang XD and Qian JC: Sotagliflozin provides additional benefits for high-fat diet-induced cardiac inflammatory injury by extra inhibiting P38MAPK and JNK. Int Immunopharmacol 155: 114631, 2025.
34. Young SL, Ryan L, Mullins TP, Flint M, Steane SE, Walton SL, Bielefeldt-Ohmann H, Carter DA, Reichelt ME and Gallo LA: Sotagliflozin, a dual SGLT1/2 inhibitor, improves cardiac outcomes in a normoglycemic mouse model of cardiac pressure overload. Front Physiol 12: 738594, 2021.
35. Bode D, Semmler L, Wakula P, Hegemann N, Primessnig U, Beindorff N, Powell D, Dahmen R, Ruetten H, Oeing C, *et al*: Dual SGLT-1 and SGLT-2 inhibition improves left atrial dysfunction in HFpEF. Cardiovasc Diabetol 20: 7, 2021.
36. Ichikawa Y, Ghanefar M, Bayeva M, Wu R, Khechaduri A, Naga Prasad SV, Mutharasan RK, Naik TJ and Ardehali H: Cardiotoxicity of doxorubicin is mediated through mitochondrial iron accumulation. J Clin Invest 124: 617-630, 2014.
37. Sawyer DB: Anthracyclines and heart failure. N Engl J Med 368: 1154-1156, 2013.
38. Simůnek T, Stérba M, Popelová O, Adamcová M, Hrdina R and Gersl V: Anthracycline-induced cardiotoxicity: Overview of studies examining the roles of oxidative stress and free cellular iron. Pharmacol Rep 61: 154-171, 2009.
39. Renu K, V G A, P B TP and Arunachalam S: Molecular mechanism of doxorubicin-induced cardiomyopathy-an update. Eur J Pharmacol 818: 241-253, 2018.
40. Christidi E and Brunham LR: Regulated cell death pathways in doxorubicin-induced cardiotoxicity. Cell Death Dis 12: 339, 2021.
41. Das J, Ghosh J, Manna P and Sil PC: Taurine suppresses doxorubicin-triggered oxidative stress and cardiac apoptosis in rat via up-regulation of PI3-K/Akt and inhibition of p53, p38-JNK. Biochem Pharmacol 81: 891-909, 2011.
42. Hanada M, Aimé-Sempé C, Sato T and Reed JC: Structure-function analysis of Bcl-2 protein. Identification of conserved domains important for homodimerization with Bcl-2 and heterodimerization with Bax. J Biol Chem 270: 11962-11969, 1995.
43. Oltvai ZN, Milliman CL and Korsmeyer SJ: Bcl-2 heterodimerizes in vivo with a conserved homolog, Bax, that accelerates programmed cell death. Cell 74: 609-619, 1993.
44. Rudel T: Caspase inhibitors in prevention of apoptosis. Herz 24: 236-241, 1999.
45. Zhang S, Liu X, Bawa-Khalfe T, Lu LS, Lyu YL, Liu LF and Yeh ET: Identification of the molecular basis of doxorubicin-induced cardiotoxicity. Nat Med 18: 1639-1642, 2012.
46. Akolkar G, da Silva Dias D, Ayyappan P, Bagchi AK, Jassal DS, Salemi VMC, Irigoyen MC, De Angelis K and Singal PK: Vitamin C mitigates oxidative/nitrosative stress and inflammation in doxorubicin-induced cardiomyopathy. Am J Physiol Heart Circ Physiol 313: H795-H809, 2017.
47. Yarmohammadi F, Karbasforooshan H, Hayes AW and Karimi G: Inflammation suppression in doxorubicin-induced cardiotoxicity: Natural compounds as therapeutic options. Naunyn Schmiedebergs Arch Pharmacol 394: 2003-2011, 2021.
48. Sun Z, Fang C, Xu S, Wang B, Li D, Liu X, Mi Y, Guo H and Jiang J: SIRT3 attenuates doxorubicin-induced cardiotoxicity by inhibiting NLRP3 inflammasome via autophagy. Biochem Pharmacol 207: 115354, 2023.
49. Zeng C, Duan F, Hu J, Luo B, Huang B, Lou X, Sun X, Li H, Zhang X, Yin S and Tan H: NLRP3 inflammasome-mediated pyroptosis contributes to the pathogenesis of non-ischemic dilated cardiomyopathy. Redox Biol 34: 101523, 2020.
50. Lebrecht D, Kokkori A, Ketelsen UP, Setzer B and Walker UA: Tissue-specific mtDNA lesions and radical-associated mitochondrial dysfunction in human hearts exposed to doxorubicin. J Pathol 207: 436-444, 2005.
51. Li J, Wang PY, Long NA, Zhuang J, Springer DA, Zou J, Lin Y, Bleck CKE, Park JH, Kang JG and Hwang PM: p53 prevents doxorubicin cardiotoxicity independently of its prototypical tumor suppressor activities. Proc Natl Acad Sci USA 116: 19626-19634, 2019.
52. Antonucci S, Di Sante M, Tonolo F, Pontarollo L, Scalcon V, Alanova P, Menabò R, Carpi A, Bindoli A, Rigobello MP, *et al*: The determining role of mitochondrial reactive oxygen species generation and monoamine oxidase activity in doxorubicin-induced cardiotoxicity. Antioxid Redox Signal 34: 531-550, 2021.
53. Kubli DA and Gustafsson AB: Mitochondria and mitophagy: The yin and yang of cell death control. Circ Res 111: 1208-1221, 2012.
54. Schirone L, D'Ambrosio L, Forte M, Genovese R, Schiavon S, Spinosa G, Iacovone G, Valenti V, Frati G and Sciarretta S: Mitochondria and doxorubicin-induced cardiomyopathy: A complex interplay. Cells 11: 2000, 2022.
55. Rodriguez C, Muñoz M, Contreras C and Prieto D: AMPK, metabolism and vascular function. FEBS J 288: 3746-3771, 2021.
56. Sciarretta S, Forte M, Frati G and Sadoshima J: New insights into the role of mTOR signaling in the cardiovascular system. Circ Res 122: 489-505, 2018.
57. Timm KN and Tyler DJ: The Role of AMPK activation for cardioprotection in doxorubicin-induced cardiotoxicity. Cardiovasc Drugs Ther 34: 255-269, 2020.
58. Zhu J, Wang YF, Chai XM, Qian K, Zhang LW, Peng P, Chen PM, Cao JF, Qin ZH, Sheng R and Xie H: Exogenous NADPH ameliorates myocardial ischemia-reperfusion injury in rats through activating AMPK/mTOR pathway. Acta Pharmacol Sin 41: 535-545, 2020.
59. Li X, Wang X, Wang B, Chi W, Li Z, Zhang M, Shen Y, Liu X, Lu Y and Liu Y: Dihydromyricetin protects against Doxorubicin-induced cardiotoxicity through activation of AMPK/mTOR pathway. Phytomedicine 99: 154027, 2022.
60. Liu D and Zhao L: Spinacetin alleviates doxorubicin-induced cardiotoxicity by initiating protective autophagy through SIRT3/AMPK/mTOR pathways. Phytomedicine 101: 154098, 2022.
61. Zhang S, Wei X, Zhang H, Wu Y, Jing J, Huang R, Zhou T, Hu J, Wu Y, Li Y and You Z: Doxorubicin downregulates autophagy to promote apoptosis-induced dilated cardiomyopathy via regulating the AMPK/mTOR pathway. Biomed Pharmacother 162: 114691, 2023.
62. Marino A, Hausenloy DJ andreadou I, Horman S, Bertrand L and Beauloye C: AMP-activated protein kinase: A remarkable contributor to preserve a healthy heart against ROS injury. Free Radic Biol Med 166: 238-254, 2021.
63. Aslam M and Ladilov Y: Emerging role of cAMP/AMPK signaling. Cells 11: 308, 2022.
64. Li X, Liu J, Lu Q, Ren D, Sun X, Rousselle T, Tan Y and Li J: AMPK: A therapeutic target of heart failure-not only metabolism regulation. Biosci Rep 39: BSR20181767, 2019.
65. Huang Q, Ren Y, Yuan P, Huang M, Liu G, Shi Y, Jia G and Chen M: Targeting the AMPK/Nrf2 pathway: A novel therapeutic approach for acute lung injury. J Inflamm Res 17: 4683-4700, 2024.
66. Song K, Kong X, Zhang Z, Xian Y, He M, Zhang Y, Liao X, Huang Z, Kang A, Xiao D and Ren Y: Sleeve gastrectomy ameliorates renal injury in obesity-combined hyperuricemic nephropathy mice by modulating the AMPK/Nrf2/ABCG2 pathway. Sci Rep 14: 22834, 2024.
67. Zimmermann K, Baldinger J, Mayerhofer B, Atanasov AG, Dirsch VM and Heiss EH: Activated AMPK boosts the Nrf2/HO-1 signaling axis-a role for the unfolded protein response. Free Radic Biol Med 88: 417-426, 2015.
68. Li S, Dong S, Xu Q, Shi B, Li L, Zhang W, Zhu J, Cheng Y, Zhang G and Zhong M: Sleeve gastrectomy-induced AMPK activation attenuates diabetic cardiomyopathy by maintaining mitochondrial homeostasis via NR4A1 suppression in rats. Front Physiol 13: 837798, 2022.
69. Peng Y, Rideout DA, Rakita SS, Gower WR, You M and Murr MM: Does LKB1 mediate activation of hepatic AMP-protein kinase (AMPK) and sirtuin1 (SIRT1) after Roux-en-Y gastric bypass in obese rats? J Gastrointest Surg 14: 221-228, 2010.

70. Goje ID, Goje GI, Ordodi VL, Ciobotaru VG, Ivan VS, Buzaș R, Tunea O, Bojin F and Lighezan DF: Doxorubicin-induced cardiotoxicity and the emerging role of SGLT2 inhibitors: From glycemic control to cardio-oncology. Pharmaceuticals (Basel) 18: 681, 2025.
71. Li J, Qiao J, Zhang S, Zhong J, Ke C, Lin Y, Li Y, Jin Y, Yao Y, Zhai A and Bi C: Unveiling the anticancer potential of SGLT-2 inhibitors: Mechanisms and prospects in clinical oncology-a narrative review. Eur J Med Res 30: 520, 2025.
72. Wang Y, Wang Z, Guo X, Tao Z, Wu C, Jiang M and Pu J: Empagliflozin attenuates DOX-induced cardiotoxicity by inhibiting RIPK1-mediated endoplasmic reticulum stress and autophagy. Biochim Biophys Acta Mol Basis Dis 1871: 167898, 2025.
73. Eliaa SG, Al-Karmalawy AA, Saleh RM and Elshal MF: Empagliflozin and doxorubicin synergistically inhibit the survival of triple-negative breast cancer cells via interfering with the mTOR pathway and inhibition of calmodulin: In vitro and molecular docking studies. ACS Pharmacol Transl Sci 3: 1330-1338, 2020.
74. Podyacheva E, Shmakova T, Kushnareva E, Onopchenko A, Martynov M, Andreeva D, Toropov R, Cheburkin Y, Levchuk K, Goldaeva A and Toropova Y: Modeling doxorubicin-induced cardiomyopathy with fibrotic myocardial damage in wistar rats. Cardiol Res 13: 339-356, 2022.
75. Medeiros-Lima DJM, Carvalho JJ, Tibirica E, Borges JP and Matsuura C: Time course of cardiomyopathy induced by doxorubicin in rats. Pharmacol Rep 71: 583-590, 2019.